# QUARK–HADRON DUALITY AT FINITE TEMPERATURE*

E. Ruiz Arriola, L.L. Salcedo

Departamento de Física Atómica, Molecular y Nuclear
and
Instituto Carlos I de Física Teórica y Computacional
Universidad de Granada, 18071 Granada, Spain

E. Megías

Grup de Física Teòrica and IFAE, Departament de Física
Universitat Autònoma de Barcelona, Bellaterra 08193 Barcelona, Spain
and
Max-Planck-Institut für Physik (Werner-Heisenberg-Institut)
Föhringer Ring 6, 80805 Munich, Germany

*(Received November 11, 2014)*

At low temperatures, we expect that all QCD observables are defined in terms of hadrons. This includes the partition function as well as the Polyakov loop in all representations. We analyze the physics underlying a microscopic derivation of the hadron resonance gas.

DOI:10.5506/APhysPolB.45.2407
PACS numbers: 12.38.Lg, 11.10.Wx, 12.38.–t

## 1. Introduction

The promise of a phase transition at finite temperature in QCD from the confined hadronic phase to a deconfined quark–gluon phase has triggered a lot of activity both theoretically as well as experimentally. This original prediction by early lattice calculations [1–3] has turned into a smooth crossover after many years of accumulated experience [4]. The determination and understanding of the QCD equation of state (EoS) from the lattice [5] plays a crucial role in the current analysis of ultra-relativistic heavy ion collisions [6].

* Invited talk presented at the LIV Cracow School of Theoretical Physics "QCD Meets Experiment", Zakopane, Poland, June 12–20, 2014.

While in the limit of massless quarks the QCD Lagrangian is scale invariant, implying a vanishing trace of the energy momentum tensor, the symmetry is broken explicitly by the finite quark masses and anomalously by the necessary renormalization which introduces an energy scale and generates a trace anomaly. The most recent up-to-date results for 2+1 flavour lattices have been obtained by the Wuppertal–Budapest(WB) [7] and HotQCD [8] collaborations, and after continued discrepancies there is a final consensus that maximal violation of scale invariance occurs at $T_{\rm s} \sim 200$ MeV where the trace anomaly reaches its maximum value.

At very high temperatures, the typical momentum scales or $\mu \sim 2\pi T$ are large and finite quark mass effects can be neglected. Due to asymptotic freedom, the strong and running coupling constant becomes small and thus interactions can be neglected. Thus, one effectively has a gas of free and massless $4N_fN_c$ fermions (quarks and antiquarks) and $2(N_c^2-1)$ bosons (gluons), and scale invariance is restored. At the same time, colour is delocalized corresponding to a deconfined phase. This allows, in principle, to count the number of $2N_fN_c$ quark and $2(N_c^2-1)$ gluon elementary species by means of the Stefan–Boltzmann law. Current analyses show that this happens for temperatures much larger than $T_{\rm s}$.

Yet, there is the firm belief that because of confinement, hadron states, composite, extended and most often unstable bound states made of quarks and gluons build a complete basis at very low temperatures, where they effectively behave as point-like, stable, non-interacting and structureless particles. This quark–hadron duality resembles to a large extent the similar duality between different degrees of freedom as the one found in deep inelastic scattering (for a review, see [9]). It is remarkable that in the large $N_c$ limit some of these requirements are indeed fulfilled (for a review, see *e.g.* [10]), except and most notably the point-like character. Of course, as the temperature is raised, we expect many excited states to contribute, but also that finite width and finite size effects play a role. How this hadronization happens in detail has not really been understood so far. Lattice calculations suggest that there is a smooth transition or crossover from the purely hadronic phase to the purely quark–gluon phase [4]. Actually, it is not obvious when this hadronic picture fails in practice or what is the main mechanism behind quark and gluon liberation at the lowest possible temperature. The present contribution tries to address this problem guided by our own experience on the field.

## 2. The hadron resonance gas

In the opposite limit of very low temperatures $T \ll T_{\rm s}$, one expects an interacting gas of the lightest colour neutral particles (for $N_f = 3$ pions and kaons) [11]. Because of the spontaneous chiral symmetry breaking, the low-

lying pseudoscalar particles are the lightest Goldstone bosons made of $u, d, s$ quarks. For the typical low momenta in the heat bath $p \sim 2\pi T \ll m_\pi, m_K$ Goldstone bosons interact weakly through derivative couplings and hence interactions are strongly suppressed. Thus, scale invariance violations of the non-interacting gas are due to the finite pion and kaon masses. Therefore, in the chiral limit of massless pseudoscalars, scale invariance is also exact at sufficiently low temperatures. Because of the small signal, current lattice calculations of the trace anomaly are just above the edge of this pion and kaon gas, which is expected to work for $T \sim m_\pi/2\pi$.

When the temperature is raised, hadronic interactions among pions start playing a role and two- and more particle states contribute to the thermodynamic properties. The calculation may be organized according to the quantum virial expansion [12] where there are two kinds of contributions. The excluded volume corrections come from repulsive interactions which prevent particles to approach each other below a certain distance. The resonance contributions stem from attractive interactions which generate states living long enough to produce pressure in the system, meaning that the resonance can hit the wall of the container before it decays. A well known example is $\pi\pi$ scattering where one has attractive and resonating states in the isospin $I = 0, 1$ corresponding to the $\sigma$ and $\rho$ resonances, whereas one has a repulsive core in the $I = 2$ exotic channel [13, 14] providing a measure of the finite pion size. Once a $\rho$ meson is created, it may interact with another pion and produce a resonance, $\rho\pi \to A_1$ (which is a $3\pi$ state) and so on. For baryons, the situation is similar, where $N\pi \to \Delta$ is a good example of a resonance contribution. This separation between attractive and repulsive contributions leaves out the residual interaction stemming from the background scattering. The Hadron Resonance Gas (HRG) corresponds to assume that all interactions among the lightest and stable particles can be described by an ideal gas of non-interacting resonances which are effectively pictured as stable, point-like and elementary particles, hence the trace anomaly is given by

$$\mathcal{A}_{\rm HRG}(T) \equiv \frac{\epsilon - 3P}{T^4} = \frac{1}{T^4} \sum_n \int \frac{d^3p}{(2\pi)^3} \frac{E_n(p) - \vec{p} \cdot \nabla_p E_n(p)}{e^{E_n(p)/T} + \eta_n} \,, \tag{1}$$

where the sum is over *all* hadronic states including spin–isospin and antiparticle degeneracies, $\eta_n = \mp 1$ for mesons and baryons respectively, $E_n(p) = \sqrt{p^2 + M_n^2}$ is the energy and $M_n$ are the hadron masses. This collection of masses is usually called the *hadron spectrum* and most often identified with the PDG compilation which represents an established consensus among particle physicists [15]. The states classification echoes the non-relativistic quark model, namely mesons are $q\bar{q}$ states and baryons $qqq$ states. Those

falling outside this category are classified as "further states". The hadron spectrum obtained from the PDG is depicted in Fig. 1 as well as its separation into mesonic and baryonic spectra.

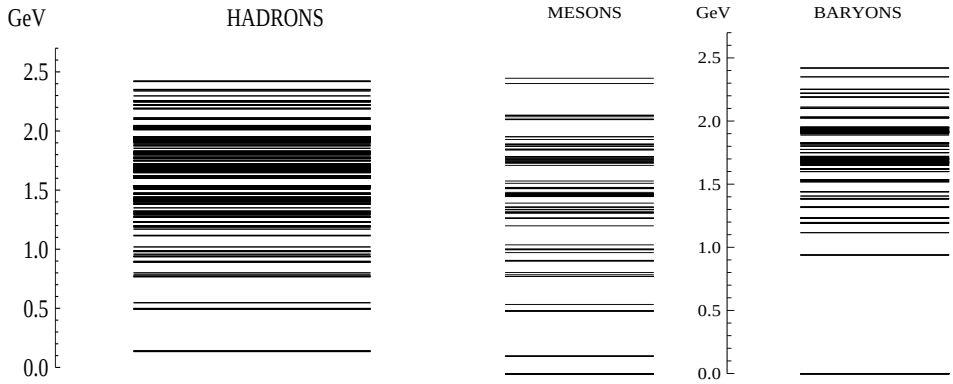


Fig. 1. Left: The full hadron spectrum made of $u$, $d$, $s$ quarks from the PDG [15]. Right: Mesonic and baryonic spectrum.

The result of using Eq. (1) with the PDG states [15] compared to the continuum extrapolated results of the Wuppertal–Budapest (WB) [7] and HotQCD [8] collaborations is shown in Fig. 2. It is amazing that this exceedingly simple picture works *accurately* almost below $T_{\rm s}$ (the maximal scale-violating temperature) at about $T \lesssim 170$ MeV. Note that the lowest lattice data points at $T = 120$ MeV are first saturated when states with masses

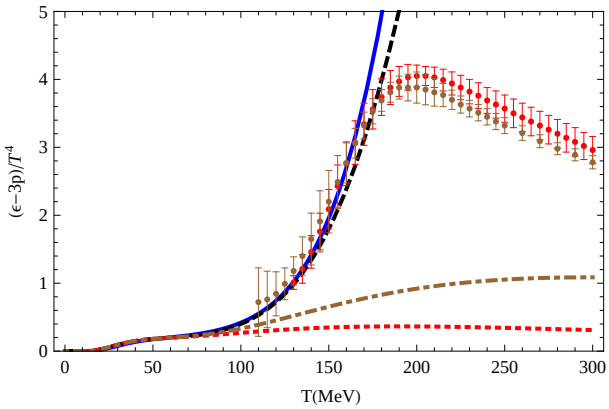


Fig. 2. Trace anomaly for the HRG using the PDG [15] (dashed) and the RQM [16, 17] (full) compared to the continuum extrapolated results of the WB [7] and HotQCD [8] collaborations. We also show the contributions from states with $M \leq 600$ MeV (dotted) and with $M \leq 800$ MeV (dot-dashed).

above the vector mesons are included. Higher temperatures start feeling excited hadronic states, which by their nature embody relativistic dynamics. The quantum statistical bosonic and baryonic character of the states accounts by less than 1% correction to the classical Maxwell–Boltzmann distribution (corresponding to take $\eta_n \to 0$) at about $T = 200$ MeV, already well beyond the range where lattice and HRG agree and much smaller than the lattice 10% uncertainties. The transition from hadrons to quarks has been analyzed on the light of strangeness [18] and an observable which vanishes for the HRG has been proposed.

Actually, the HRG model has arbitrated the discrepancies between the different collaborations in the past and the lattice community have had a long struggle until agreement *between them* and *with the HRG model* has been declared. While this has made the HRG model a sort of holy grail (see *e.g.* [19] and references therein), it is good to remind that despite of the phenomenological success it is not a theorem, nor a well defined approximation from the original QCD Lagrangian. The most compelling argument is that it is to date unclear how corrections to this simple approach should be implemented nor what the error estimate for the HRG should be. For a comparison, we also show the result of Eq. (1) using instead the Relativized Quark Model (RQM) [16, 17] which essentially combines two basic elements, the static energy among the constituents and a relativistic form of the kinetic energy which does not consider the spin of the particles but does not contain more parameters than QCD itself. The likewise impressive agreement of the RQM trace anomaly with the lattice data not only illustrates our point on the lack of uniqueness of what is actually being checked by these comparisons, but also that the RQM may provide information not listed in the PDG booklet.

For instance, the PDG lists the quantum numbers, decay modes, masses and widths of the resonances building the hadron spectrum, but no information on their size is provided. While for unstable particles this is a problematic issue (see *e.g.* [20] and references therein), within the heavy-ion literature the assumption of a constant volume is frequently made (see *e.g.* [21]). This information can be accessed by means of quark models or lattice calculations. On the other hand, as discussed in Ref. [22], the purely resonance character makes the very definition of the mass ambiguous, and this allows to generate an error band on the PDG prediction of the HRG model which gives a spread for the trace anomaly about half the lattice uncertainties.

## 3. QCD at finite temperature

As a guideline, let us provide some of the main features of QCD at finite temperature emphasizing some relevant aspects for the discussion. Many gaps in this sketchy presentation may be filled by consulting *e.g.* [5] and ref-

erences therein. The QCD Lagrangian (in Euclidean space time) is given by

$$\mathcal{L}_{\rm QCD} = -\tfrac{1}{4} G^a_{\mu\nu} G^a_{\mu\nu} + \sum_f \overline{q}^a_f \left( i\gamma_\mu D_\mu - m_f \right) q^a_f \,. \tag{2}$$

The QCD Lagrangian is invariant under colour gauge transformations

$$\begin{aligned} q(x) &\to e^{i\sum_a (\lambda_a)^c \alpha_a(x)} q(x) \equiv \omega(x) q(x) \,, \\ A_\mu(x) &\to \omega^{-1}(x) A_\mu(x) \omega(x) + \frac{i}{g} \omega^{-1}(x) \partial_\mu \omega(x) \,. \end{aligned}$$

The QCD thermodynamics is obtained from the partition function

$$\begin{aligned} Z_{\rm QCD} &= {\rm Tr}\, e^{-H/T} = \sum_n e^{-E_n/T} \\ &= \int \mathcal{D} A_{\mu,a} \exp\left[ -\tfrac{1}{4} \int d^4x \left( G^a_{\mu\nu} \right)^2 \right] {\rm Det}\left( i\gamma_\mu D_\mu - m_f \right) \,, \end{aligned}$$

with the periodic or anti-periodic boundary conditions for gluons and quarks respectively

$$q(\vec{x}, \beta) = -q(\vec{x}, 0) \,, \qquad A_\mu(\vec{x}, \beta) = A_\mu(\vec{x}, 0) \,, \qquad \beta = 1/T \,,$$

$$\int \frac{dp_0}{2\pi} f(p_0) \to T \sum_n f(w_n) \,,$$

where the Matsubara frequencies are $w_n = 2n\pi T$ for gluons and $w_n = (2n+1)\pi T$ for quarks. Preservation of the quark antiperiodic boundary conditions implies that only periodic gauge transformations are allowed, namely

$$\omega(\vec{x}, x_0 + \beta) = \omega(\vec{x}, x_0) \,, \qquad \beta = 1/T \,. \tag{3}$$

Within the convenient Polyakov gauge ($A_0(x)$ stationary and everywhere diagonal [23]), the most general remaining transformation is either stationary and diagonal or of the type

$$\omega(x_0) = e^{i 2\pi x_0 \lambda/\beta} \,, \tag{4}$$

where $\lambda = {\rm diag}(n_1, \cdots, n_{N_c})$ and ${\rm Tr}\,\lambda = 0$. Large gauge invariance implies periodicity in $A_0$ with period $2\pi T/g$

$$A_0 \to A_0 - \frac{2\pi T}{g} \lambda \,. \tag{5}$$

This is the finite temperature version of the Gribov copies, *i.e.*, the fact that there is no complete gauge fixing in a non-Abelian gauge theory. A drastic

consequence of this periodicity property is that it becomes explicitly broken in perturbation theory [24, 25]. Thus, we may consider this as a signal of the relevance of non-perturbative finite temperature gluons.

In the limit of massless quarks ($m_f = 0$), the QCD Lagrangian is scale invariant, *i.e.* $x \longrightarrow \lambda x$. This symmetry is broken by quantum corrections due to the necessary regularization. To see this, consider the partition function dependence on the coupling constant $g$ after the rescaling of the gluon field $\bar{A}_\mu = gA_\mu$ (and ignoring renormalization issues)

$$Z = \int \mathcal{D}\bar{A}_{\mu,a} \exp\left[-\frac{1}{4g^2}\int d^4x \left(\bar{G}^a_{\mu\nu}\right)^2\right] \mathrm{Det}(i\gamma_\mu D_\mu)\,. \tag{6}$$

Note that the *only* dependence on $g$ is the one shown explicitly. Thus,

$$\frac{\partial \log Z}{\partial g} = \frac{1}{2g^3}\left\langle \int d^4x \left(\bar{G}^a_{\mu\nu}\right)^2 \right\rangle = \frac{1}{2g}\frac{V}{T}\left\langle \left(G^a_{\mu\nu}\right)^2 \right\rangle_T\,, \tag{7}$$

where in the last equation we have assumed a vacuum space time independent configuration, with $V$ the volume of the system. On the other hand, the free energy and internal energy are given by the thermodynamic relations

$$F = -PV = -T\log Z\,, \qquad \epsilon = \frac{E}{V} = \frac{T^2}{V}\frac{\partial \log Z}{\partial T}\,, \tag{8}$$

and the trace anomaly becomes

$$\epsilon - 3P = T^5 \frac{\partial}{\partial T}\left(\frac{P}{T^4}\right)\,. \tag{9}$$

Generally, a renormalization scale $\mu$ has to be introduced to handle both IR and UV divergences. Thus, on purely dimensional grounds, one has

$$\frac{P}{T^4} = f\big(g(\mu), \log(\mu/2\pi T)\big)\,. \tag{10}$$

Physical results should not depend on the renormalization scale, thus using that $dP/d\mu = 0$, we get

$$\frac{\partial}{\partial \log T}\left(\frac{P}{T^4}\right) = \frac{\partial g}{\partial \log \mu}\frac{\partial}{\partial g}\left(\frac{P}{T^4}\right)\,. \tag{11}$$

Introducing the beta function

$$\beta(g) = \mu\frac{dg}{d\mu} = -\beta_0 g^3 + \mathcal{O}\left(g^5\right)\,, \qquad \beta_0 = \frac{11N_c - 2N_f}{48\pi^2}\,, \tag{12}$$

the trace anomaly becomes then

$$\epsilon - 3P = \langle G^2 \rangle_T - \langle G^2 \rangle_0 \qquad \text{(massless quarks)}\,, \tag{13}$$

where

$$G^2 = \frac{\beta(g)}{2g} \left(G^a_{\mu\nu}\right)^2 . \tag{14}$$

Here we have implemented, in full harmony with standard lattice practice (see, *e.g.*, [26]), a subtraction to renormalize the vacuum contribution [27, 28]. The vanishing of the trace anomaly at zero temperature is consistent with quark–hadron duality, see Eq. (1).

Also in the massless quark limit, the QCD Lagrangian is invariant under $\mathrm{SU_R}(N_f) \times \mathrm{SU_L}(N_f)$ chiral transformations

$$q(x) \to e^{i \sum_a (\lambda_a)^f \alpha_a} q(x)\,, \qquad q(x) \to e^{i \sum_a (\lambda_a)^f \alpha_a \gamma_5} q(x)\,. \tag{15}$$

Chiral symmetry is spontaneously broken by the chiral condensate in the vacuum down to $\mathrm{SU_V}(N_f)$

$$\langle \bar{q} q \rangle \neq 0\,. \tag{16}$$

The Gell-Mann–Oakes–Renner relation, which in the simplest $N_f = 2$ case becomes

$$2 \langle \bar{q} q \rangle m_q = -f_\pi^2 m_\pi^2\,, \tag{17}$$

relates the quark condensate and the quark mass to physically measurable quantities such as the pion mass $m_\pi$ and the pion weak decay constant $f_\pi$. This relation exemplifies the *quark–hadron duality*, namely the fact that, in the confined phase of QCD, we expect quark observables to be representable by hadronic observables.

In the opposite limit that all quarks become infinitely massive, $m_f \to \infty$, the quark determinant becomes a constant which can be factored out of the path integral

$$Z_{\mathrm{QCD}} \to Z_{\mathrm{YM}} \mathrm{Det}\left(-m_f\right)\,, \tag{18}$$

and the resulting action corresponds to a pure Yang–Mills theory

$$Z_{\mathrm{YM}} = \int \mathcal{D}A_{\mu,a} \exp\left[-\tfrac{1}{4} \int d^4x \left(G^a_{\mu\nu}\right)^2\right] . \tag{19}$$

This purely gluonic action exhibits a larger symmetry: 't Hooft Center Symmetry $\mathbb{Z}(N_c)$, namely, invariance under gauge transformations which are periodic modulo a center element of $\mathrm{SU}(N_c)$

$$\omega(\vec{x}, x_0 + \beta) = z\,\omega(\vec{x}, x_0)\,, \qquad z^{N_c} = 1 \quad (z \in \mathbb{Z}(N_c))\,. \tag{20}$$

An example for $z = e^{i2\pi k/N_c}$ and in the Polyakov gauge is given by the choice

$$\omega(x_0) = e^{i2\pi x_0 k\lambda/(N_c\beta)}\,, \qquad A_0 \to A_0 - \frac{2\pi T}{gN_c} k\lambda \tag{21}$$

with $\lambda = \mathrm{diag}(1 - N_c, 1, \ldots, 1)$. The Polyakov loop is an order parameter of the center symmetry which is related to the free energy of a colour charge in the medium. In the Polyakov gauge, the Polyakov loop in the fundamental representation reads

$$\Omega_F(\vec{x}\,) = e^{igA_0(\vec{x}\,)/T}\,, \qquad A_0 = \sum_{a=1}^{N_c^2-1} \lambda_a A_0^a\,. \tag{22}$$

The vacuum expectation value of the Polyakov loop transforms under the previous gauge transformation as

$$L_T = \left\langle \mathrm{Tr}_c e^{igA_0/T} \right\rangle = e^{-F_q/T} \;\longrightarrow\; zL_T\,. \tag{23}$$

Therefore, unbroken symmetry ($L_T = zL_T$)) implies $L_T = 0$ and hence $F_q = \infty$. The divergence of the free energy of a colour charge in the fundamental representation is interpreted as a signal for confinement [29]. The renormalization of the Polyakov loop is a subtle issue addressed in the lattice in Ref. [30].

In gluodynamics, the center symmetry is spontaneously broken above a critical temperature and $L_T/N_c$ approaches unity (or any other central element) as the temperature increases. In fact, at high temperatures $A_0 \ll T$ and one may expand [31]

$$\frac{1}{N_c} L_T = 1 - \frac{g^2 \left\langle \mathrm{Tr}_c A_0^2 \right\rangle}{2N_c T^2} + \cdots = e^{-\frac{g^2 \left\langle \mathrm{Tr}_c A_0^2 \right\rangle}{2N_c T^2} + \cdots}\,. \tag{24}$$

Note that while this formula suggests that $L_T \leq N_c$, the renormalization overshoots this value at a perturbative level in a tiny but visible way [31–33].

In full QCD, the center symmetry is explicitly broken, which results in $L_T > 0$ at all temperatures. In the limit of heavy quarks and low temperature, one has $L_T = \mathcal{O}(e^{-m_q/T}) \ll 1$ or $F_q \to m_q + \epsilon + \ldots$, where $\epsilon$ is the smallest residual binding energy of doubly heavy $Q\bar{Q}$ meson. Likewise for light dynamical quarks $L_T \sim e^{-\Delta/T}$, where $\Delta$ denotes the ground state mass of a heavy–light $Q\bar{q}$ meson (the mass of the heavy quark excluded) [34].

One can also define Polyakov loops in higher representations which have been subject of attention only a few times despite its very interesting properties [35–38].

Scale invariance is also broken in gluodynamics. For instance, in perturbation theory to two loops, one has [39]

$$\mathcal{A} \equiv \frac{\epsilon - 3P}{T^4} = \frac{N_c\left(N_c^2-1\right)}{72}\beta_0 g(T)^4 + \mathcal{O}\left(g^5\right) , \tag{25}$$

where at the lowest order

$$\frac{1}{g(\mu)^2} = \beta_0 \log\left(\mu^2/\Lambda^2_{\rm QCD}\right) . \tag{26}$$

Thus, taking $\mu = 2\pi T$, we expect to have a free gas of gluons and quarks in the high temperature limit. In the simple case of non-interacting particles, the partition function is given by

$$\log Z = V\eta g_i \int \frac{d^3p}{(2\pi)^3} \log\left[1+\eta e^{-E_p/T}\right] , \qquad E_p = \sqrt{p^2+m^2} , \tag{27}$$

where $\eta = -1$ for bosons, $\eta = +1$ for fermions and $g_i$ is the number of species. From the partition function, we have the thermodynamic identities

$$\begin{aligned} F &= -T\log Z , & P &= -\frac{\partial F}{\partial V} , \\ S &= -\frac{\partial F}{\partial T} , & E &= F + TS . \end{aligned}$$

For the massless quark and gluon gas, the pressure is given by

$$P = \left[2\left(N_c^2-1\right) + 4N_cN_f\frac{7}{8}\right]\frac{\pi^2}{90}T^4 , \tag{28}$$

which is the Stefan–Boltzmann law. Since in the high temperature limit the particles are effectively massless, scale invariance is restored and hence the (reduced) trace anomaly vanishes

$$\mathcal{A} \equiv \frac{\epsilon - 3P}{T^4} \to 0 \qquad (T\to\infty) . \tag{29}$$

These expectations have been checked in Ref. [40] by a lattice study in a wide temperature window, $T = 0.7\ldots 10^3 T_{\rm c}$.

Thus, the quark condensate $\langle\bar{q}q\rangle$ and the Polyakov loop in the fundamental representation $L_T$ become true order parameters in quite opposite situations. While $\langle\bar{q}q\rangle$ signals spontaneous chiral symmetry breaking in the massless quark limit, $L_T$ signals confinement for infinitely heavy quarks. The real situation is somewhat intertwined, and can be summarized as follows.

— Order parameter of chiral symmetry breaking ($m_q = 0$)
Quark condensate $\mathrm{SU_R}(N_f) \times \mathrm{SU_L}(N_f) \to \mathrm{SU_V}(N_f)$

$$\langle \bar{q}q \rangle \neq 0 \quad (T < T_\mathrm{c}) \,, \qquad \langle \bar{q}q \rangle = 0 \quad (T > T_\mathrm{c}) \,.$$

— Order parameter of deconfinement ($m_q = \infty$)
Polyakov loop: Center symmetry $\mathbb{Z}(N_c)$ broken

$$L_T = 0 \quad (T < T_\mathrm{c}) \,, \qquad L_T > 0 \quad (T > T_\mathrm{c}) \,.$$

— In the real world, $m_q$ is finite but inflection points nearly coincide (accidental?)

$$\frac{d^2}{dT^2} L_T = 0 \,, \qquad \frac{d^2}{dT^2} \langle \bar{q}q \rangle_T = 0 \,,$$

at about the same temperature $T_\mathrm{c} = 155(10)$ MeV.

The chiral-deconfinement crossover is a unique prediction of lattice QCD. Whether or not this result is accidental, could be answered by computing the (connected) crossed correlator,

$$\left\langle \bar{q}q \, \mathrm{Tr}_c \, e^{igA_0/T} \right\rangle - \langle \bar{q}q \rangle \left\langle \mathrm{Tr}_c \, e^{igA_0/T} \right\rangle = \frac{\partial L_T}{\partial m_q} \,, \tag{30}$$

which corresponds to the quark mass dependence of the Polyakov loop.

Finally, the correlation function between Polyakov loops in an arbitrary representation $R$ exhibits Casimir scaling (quenched approximation) [41]

$$\left\langle \mathrm{Tr}_R \Omega(\vec{x}_1) \mathrm{Tr}_R \Omega(\vec{x}_2)^\dagger \right\rangle \approx e^{-\sigma_R |\vec{x}_1 - \vec{x}_2|/T} \,, \qquad \sigma_R = (C_R/C_F) \, \sigma_F \,. \tag{31}$$

It can be shown that this correlation function, which for the fundamental representation is related to the $\bar{q}q$ free energy, $F_1(r,T)$, can also be written as a ratio of partition functions between $\bar{Q}Q$ sources placed at a distance $|\vec{x}_1 - \vec{x}_2|$ and the vacuum [42], hence satisfying a spectral decomposition with integral weights $w_n$ and positive energies $E_n(|\vec{x}_1 - \vec{x}_2|) > 0$,

$$\left\langle \mathrm{Tr}_F \Omega(\vec{x}_1) \mathrm{Tr}_F \Omega(\vec{x}_2)^\dagger \right\rangle = \sum_n w_n e^{-E_n(|\vec{x}_1 - \vec{x}_2|)/T} = e^{-F_1(r,T)/T} \,, \tag{32}$$

where the free energy $F_1(r,T)$ has been introduced. One important property is that at large distances (for the unquenched full QCD case)

$$\left\langle \mathrm{Tr}_F \Omega(\vec{r}) \mathrm{Tr}_F \Omega(0)^\dagger \right\rangle \to |\langle \mathrm{Tr}_F \Omega \rangle|^2 = L_T^2 \,. \tag{33}$$

## 4. Relativized quark–gluon models

### *4.1. Relativity and thermodynamics*

One of the most troublesome aspects of hadron binding is that it makes relatively heavy particles from massless ones, hence most of the mass comes from the interaction. A prominent example is the glueball in gluodynamics, where the lightest $0^{++}$ state [43] has a mass $M_{0^{++}}/\sqrt{\sigma} \sim 4.5$, while gluons are massless. Fully relativistic few body equations are not only hard to handle but encounter many difficulties regarding cluster decomposition properties [44–46]. This feature is particularly interesting as it is related to the compositeness nature of relativistic particles which build the hadrons, and, strictly speaking, we have to deal with relativistic statistical mechanics of interacting particles, a subject which has a long history [47].

Unfortunately, as we have shown, the physics of finite temperature QCD below the phase transition involves the excited hadronic spectrum, and thus relativity becomes an essential ingredient in the game. Relativized quark models (RQM) combine two basic elements, the static energy among the constituents and a relativistic form of the kinetic energy which does not consider the spin of the particles [16, 17].

### *4.2. The linear potential*

In the Born–Oppenheimer approximation, the object to be analyzed is the interaction between heavy sources $A$ and $B$. In perturbation theory, one has one gluon exchange which yields a Coulomb like interaction,

$$V_{AB}(r) = \lambda_A \, \lambda_B \frac{\alpha_{\rm s}}{r} \, , \tag{34}$$

where $\alpha_{\rm s} = g^2/(4\pi)$ and $\lambda_A$ and $\lambda_B$ are the generators[1] of the SU(3) colour group corresponding to the representation of the source. This form of the colour interaction exhibits Casimir scaling, a property that is violated only at three loops in perturbation theory [48] and appears to hold non-perturbatively on the lattice with an additional linear potential contribution [49]. Thus, to a good approximation, the interaction between heavy sources on the lattice reads

$$V_{AB}(r) = \lambda_A \, \lambda_B \left[ \frac{\alpha_{\rm s}}{r} - \kappa r \right] \, . \tag{35}$$

Thus, for quark–antiquark or gluon–gluon pairs coupled to a singlet state or a quark–quark pair coupled to the antifundamental representation (diquark),

[1] These are more customarily denoted by $T$, while $\lambda$ is twice the generator.

the following relations are obtained:

$$V_{Q\bar{Q}}(r) \;=\; \sigma_F\, r - \frac{4\alpha_{\rm s}}{3r} + \cdots\,, \tag{36}$$

$$V_{GG}(r) \;=\; \sigma_A\, r - \frac{3\alpha_{\rm s}}{r} + \cdots\,, \tag{37}$$

$$V_{QQ}(r) \;=\; \sigma_d\, r - \frac{2\alpha_{\rm s}}{3r} + \cdots\,. \tag{38}$$

In what follows, we use $\sigma$ to denote the string tension $\sigma_F$. As a consequence of the Casimir scaling, the ratio between the fundamental $Q\bar{Q} \equiv (\mathbf{3}\times\bar{\mathbf{3}})_{\mathbf{1}}$, adjoint $GG \equiv (\mathbf{8}\times\mathbf{8})_{\mathbf{1}}$, and diquark $QQ \equiv (\mathbf{3}\times\mathbf{3})_{\bar{\mathbf{3}}}$ colour sources are

$$\frac{\sigma_A}{\sigma_F} = \frac{9}{4}\,, \qquad \frac{\sigma_d}{\sigma_F} = \frac{1}{2}\,. \tag{39}$$

By making simplifying assumptions, easy relations can be derived from the Casimir scaling. For instance, consider the lowest glueball state by analyzing two massless spin-1 particles in the CM system assuming spin-independent interactions, and similarly for the $\rho$ meson as composed of two massless quarks. Neglecting the Coulomb term, the respective mass operators appearing in the Salpeter equation read

$$\hat{M}_G = 2p + \sigma_A\, r\,, \qquad \hat{M}_M = 2p + \sigma_F\, r\,. \tag{40}$$

Simple dimensional considerations imply that the eigenmasses are proportional to the square root of the string tension, thus

$$M_{g,0^{++}}/m_\rho \approx 3/2\,.$$

Here, as it is customary, we have matched the scales of gluodynamics and QCD by assuming a common value of $\sigma_F$ in both theories. A rough estimate of the mass follows from using the uncertainty principle for the ground state, namely, by taking $pr \sim 1$. For the glueball, this yields

$$M_0 \approx \min\left[\frac{2}{r} + \sigma_A\, r\right] = 2\sqrt{2\sigma_A} = 4.2\sqrt{\sigma}\,.$$

### *4.3. The cumulative number*

The spectrum of the RQM model of Isgur and collaborators for $\bar{q}q$ in the case of mesons and $qqq$ for baryons [16, 17] is concisely shown in Fig. 3. A detailed comparison to individual states unveils a rather good description of the data. Of course, we do not expect this or any quark model Hamiltonian

to describe accurately the individual levels. This, however, poses an interesting problem on how two different spectra including many excited states can quantitatively be compared, beyond eyesight and subjective impression just based on contemplating Figs. 1 and 3. One way suggested by Hagedorn in the early 60s is by means of the cumulative number of states

$$N(M) = \sum_n \theta(M - M_n)\,. \tag{41}$$

The question is then to decide to *what* extent $N_{\rm QCD}(M)$ or $N_{\rm PDG}(M)$ coincide.

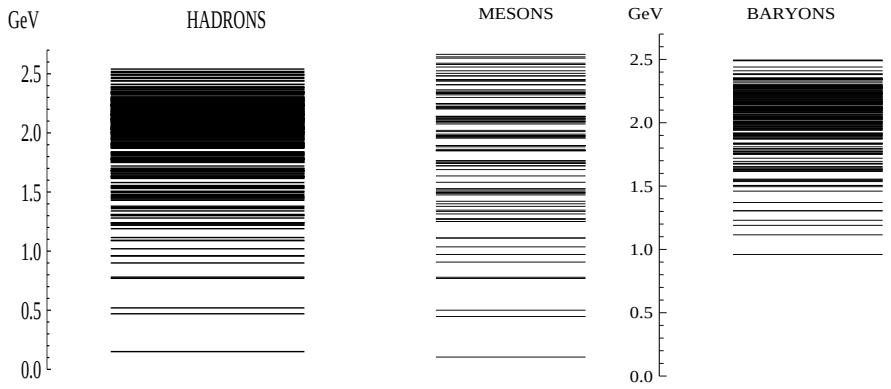


Fig. 3. Left: The full hadron spectrum made of $u, d, s$ quarks from the Relativized Quark Model (RQM) of Isgur and collaborators where mesons are described as bound $\bar{q}q$ states and baryons as bound $qqq$ states [16, 17]. Right: Mesonic and baryonic spectrum.

For our discussion, we will consider a simplified version of that model where hyperfine splittings due to spin and three-body forces are ignored and the Hamiltonian for $n$ constituents (we restrict to $q\bar{q}$ and $qqq$ systems) is taken to be

$$H_n = \sum_{i=1}^{n} \sqrt{p_i^2 + m_i^2} - \sum_{i<j} \lambda_i\,\lambda_j v(r_{ij})\,, \qquad v(r) = \kappa\, r - \frac{\alpha_{\rm s}}{r}\,. \tag{42}$$

We will consider explicitly some cases of interest below, but already at this level some important observations can be made on the growth of the cumulative number of states. To this end, let us adopt a semiclassical approximation, which should be reliable when the number of states is large. The number of states in the CM system and at rest, below a certain mass $M$

takes the form

$$N_n(M) \sim g_n \int \prod_{i=1}^{n} \frac{d^3x_i d^3p_i}{(2\pi)^3} \delta^{(3)}\left(\sum_{i=1}^{n} \vec{x}_i\right) \delta^{(3)}\left(\sum_{i=1}^{n} \vec{p}_i\right) \theta(M - H_n)\,, \quad (43)$$

where $g_n$ takes into account the degeneracy. For the sake of the argument, let us neglect the Coulomb term, thus $v(r) = \kappa\, r$, as well as the current quark masses. In this case, a dimensional argument, $p \to Mp$, $r \to Mr/\kappa$, gives

$$N_n(M) \sim \left(\frac{M^2}{\kappa}\right)^{3n-3}. \quad (44)$$

It is not hard to show that lifting any of the above approximations only modifies this result by subleading powers of $M$. Thus, for a finite number of degrees of freedom, the leading contribution to the cumulative number scales as a power of the mass. The qualitative power behaviour can be clearly identified as straight lines in the log–log plot of Fig. 4 for the cumulative number, where we compare the resulting cumulative number both for the PDG and the RQM separating the mesonic and baryonic contributions.

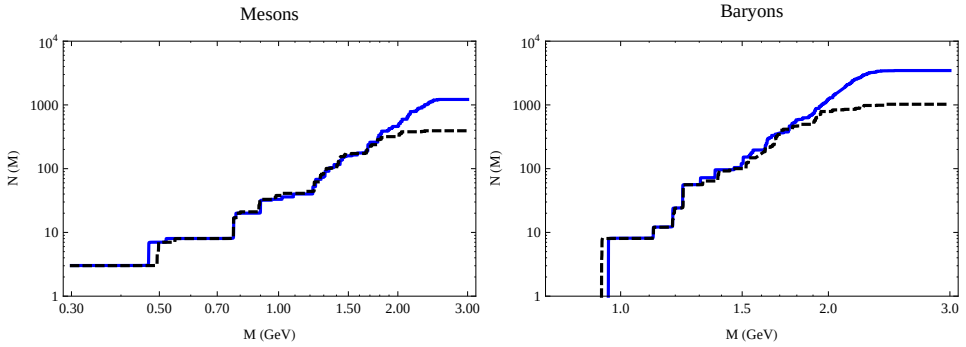


Fig. 4. Cumulative numbers for the PDG (dashed line) and the RQM (full line). Left panel: Mesonic states (log–log scale). Right panel: Baryonic states (log–log scale).

As we can also see, the PDG and RQM spectra look very much alike below 1.7–1.8 GeV. We note, however, that the spectrum for the RQM saturates sharply at 2.5 GeV which is about the cut-off mass where Isgur, Godfrey and Capstick stopped to compute states. On the other hand, the PDG states saturate at lower energy values in a softer fashion. Note that the RQM looks like a linear extrapolation (mind the log scale) of the PDG spectrum. The agreement at lower masses is not highly surprising since

RQM parameters were tuned to reproduce low lying states on the one side *and* the listed PDG states fit into the quark model scheme on the other side. On the other hand, there are only $\sigma$ and the $u, d, s$ quark masses as fitting parameters, so we should regard the agreement as a further big success of the RQM from a global point of view.

### *4.4. Bound states versus resonances*

One issue which is problematic from the start is that *if* $N(M)$ really counts the number of bound states, then we expect it to be, for $N_f = 2$ flavours, just pions $(\pi^+, \pi^-, \pi^0)$, nucleons $(p, n)$ and anti-nucleons $(\bar{p}, \bar{n})$, so $N(\infty) = 3+2\times 2\times 2 = 11$. More generally, we have $N(\infty) = (N_f^2-1)+2\times 2\times N_f(N_f^2-1)/3$ low lying mesons and baryons, while in the RQM $N(M)$ diverges as a power.

The cumulative number is by its own staircase nature a piecewise discontinuous function, but as we go to higher states the discontinuities smooth out. This becomes particularly visible in the RQM in the range of 2 GeV $<$ $M$ $<$ 2.5 GeV.

In addition, while in the PDG we have an issue regarding completeness of states, in the RQM case this is not the case; besides angular and spin flavour quantum numbers, the radial number can just be checked with the oscillation theorem, in the $\bar{q}q$ case, or simply by diagonalizing in a complete basis of normalizable states; no state will be left out in the process. In the PDG however, it is unclear if there are missing or redundant states although the consensus of listing states fitting into the quark model makes this argument into a circular one.

Of course, the meaning of $M_n^{\rm PDG}$ and $M_n^{\rm RQM}$ is different. While in the PDG listing, we usually encounter a Breit–Wigner resonance parameterization characterized by a mass and a width, in the RQM we have just the mass of a bound $q\bar{q}$ or $qqq$ state. We expect that when we couple these bound states obtained from the RQM to the continuum there will be, besides a width, a mass shift $M_n^{\rm RQM} \to M_n^{\rm RQM} + \Delta M_n$, whence the cumulative number for bound states will generally differ as the one for Breit–Wigner resonances, but the sign of $\Delta M_n$ is *a priori* unknown.

### *4.5. Hadron sizes*

The solution of the multiparton Hamiltonian Eq. (42) onto colour singlet states yields the corresponding hadron wave functions. To estimate the hadron size, we can make use of the virial theorem based on stationarity of eigenstates under unitary coordinate scaling $\vec{r}_i \to \lambda \vec{r}_i$ around the $\lambda = 1$ value, $\Psi(\vec{x}_1, \ldots, \vec{x}_n) \to \lambda^{3n/2}\Psi(\lambda\vec{x}_1, \ldots, \lambda\vec{x}_n)$. For light quarks we may, for simplicity, take the massless quark limit $m_q \to 0$. Thus, for the various

terms in the Hamiltonian $\langle p_i\rangle \to \langle p_i\rangle/\lambda$, likewise $\langle 1/r_{ij}\rangle \to \langle 1/r_{ij}\rangle/\lambda$ and $\langle r_{ij}\rangle \to \lambda\langle r_{ij}\rangle$, where $\langle r_{ij}\rangle$ is the mean distance between particles $i$ and $j$. Due to the virial theorem, we have for a multiparton state

$$M = -2\kappa \sum_{i<j} \lambda_i\, \lambda_j \langle r_{ij}\rangle\,. \tag{45}$$

In particular,

$$M_{\bar{q}q} = 2\sigma\langle r_{\bar{q}q}\rangle\,, \qquad M_{qqq} = \sigma\langle r_{12}+r_{13}+r_{23}\rangle = 3\sigma\langle r_{qq}\rangle \tag{46}$$

for mesons and baryons respectively. So, in this model, the size of a hadron grows *linearly* with the mass per constituent. For instance, from the relations $m_\rho = 2\sigma\langle r_{\bar{q}q}\rangle_\rho$ and $M_N = 3\sigma\langle r_{qq}\rangle_N$, we have $\langle r_{\bar{q}q}\rangle_\rho = 0.42$ fm and $\langle r_{qq}\rangle_N = 0.52$ fm. From $M_N/m_\rho = 3/2$, we would get $\langle r_{\bar{q}q}\rangle_\rho = \langle r_{qq}\rangle_N$ so we can identify the constituent quark mass as $M_q = \sigma\langle r\rangle$. Note that the above virial relation includes the Coulomb like contribution $-\alpha_{\rm s}/r$, since this term scales exactly as the kinetic piece. In the case of hadrons with one heavy quark, the virial theorem yields $M_{\bar{q}Q} = 2\sigma\langle r_{qQ}\rangle + m_Q$ and $M_{qqQ} = 2\sigma\langle r_{qQ}\rangle + \sigma\langle r_{qq}\rangle + m_Q$.

### *4.6. String breaking*

Confinement is often attributed to this ever-linear growing of the energy with the distance. This is true on the lattice only in the quenched approximation, where quark–antiquark creation is suppressed. In full QCD however, the string breaks, a fact that has been observed by lattice calculations at a distance $r_{\rm c} = 1.25$ fm [50]. This happens when a light $\bar{q}q$ pair is created in between the heavy quark and antiquark sources $Q\bar{Q}$, thus two colour singlet $\bar{q}Q$ and $\bar{Q}q$ mesonic states can be created. On the other hand, charge conjugation implies that the binding energy of the $\bar{q}Q$ and the $\bar{Q}q$ is the same and equals the residual energy of a heavy–light meson with total mass $M_{\bar{q}Q}$. Thus, the string breaking distance corresponds to

$$\sigma r_{\rm c} = 2\Delta\,, \qquad \Delta \equiv \Delta_{\bar{q}Q} = \Delta_{\bar{Q}q} = \lim_{m_Q\to\infty}(M_{\bar{q}Q} - m_Q)\,. \tag{47}$$

Good approximations to these states exist in nature for $q = u, d$ and $Q = c, b$. From heavy-quark QCD, we expect a universal (independent of the heavy-quark spin and flavour) spectrum $\Delta_{h,\alpha}$ of hybrid hadron masses (heavy-quark mass subtracted). For the lightest, pseudoscalar, hybrid meson, the following sequence should approach a value of $\Delta$, for increasingly heavier quarks and using the PDG values in the $\overline{\rm MS}$-scheme

$$\begin{aligned} M_K - m_s \equiv \Delta_s &= 396(24)\ \text{MeV}\,,\\ M_D - m_c \equiv \Delta_c &= 603(81)\ \text{MeV}\,,\\ M_B - m_b \equiv \Delta_b &= 1040(130)\ \text{MeV}\,, \end{aligned} \tag{48}$$

which gives the estimate for $r_c = 2$ fm. Another estimate can be made based on a constituent quark model picture where the total mass of the quark is $M_q = M_0 + m_q$, with $M_0$ the constituent quark mass and $m_q$ the current quark mass. Spontaneous breaking of chiral symmetry implies that in the chiral limit (massless current quark masses, $m_q \to 0$) the total mass is non-vanishing, thus $M_0 \neq 0$. Actually, for light $u, d$ mesons, current masses can be neglected. Then, the light $\bar{q}q$ meson has a mass $M_{\bar{q}q} = 2M_q$ and the mass of the light $qqq$ baryon is $M_{qqq} = 3M_q$. The mass of a heavy–light meson would then be $M_{\bar{q}Q} = M_q + M_Q = 2M_0 + m_q + m_Q$ hence $\sigma r_c = 4M_0 + 2m_q$, which for $\sqrt{\sigma} = 420$–$440$ MeV and $M_0 = 300$–$350$ MeV yields the estimate $r_c = 1.2$–$1.5$ fm for the string breaking distance, a quite reasonable value.

### *4.7. Avoided crossings*

The observation of string breaking for a $\bar{Q}Q$ system requires taking into account the mesonic $\bar{M}M$ channels into which the system may decay after $\bar{q}q$ pair creation from the vacuum. This coupled channel dynamics spans the Hilbert space $\mathcal{H} = \mathcal{H}_{\bar{Q}Q} + \mathcal{H}_{\bar{Q}q\bar{q}Q}$ and features the avoided crossing phenomenon familiar from molecular physics in the Born–Oppenheimer approximation [51]. For two channels, say $\bar{Q}Q$ and $\bar{M}M = \bar{Q}q\bar{q}Q$, one can compute the *direct* correlators yielding the lowest energies

$$V_{\bar{Q}Q}(r) = \sigma r\,, \qquad V_{\bar{Q}q\bar{q}Q}(r) = \Delta_{\bar{q}Q} + \Delta_{\bar{Q}q} \equiv 2\Delta\,. \tag{49}$$

These two channels are orthogonal for all $r$. For simplicity, we have disregarded the Coulomb piece $-4\alpha_s/3r$ as well as the residual interaction between the two heavy–light mesons $M = \bar{q}Q$ and $\bar{M} = \bar{Q}q$ which is of van der Waals type and corresponds to meson exchange. Note that these curves cross when $\sigma r_c = 2\Delta$. Thus, the spectrum in the Hilbert space with $\bar{Q}Q$ and $\bar{M}M = \bar{Q}q\bar{q}Q$ components reads

$$E_0(r) = \sigma r\theta(r_c - r) + 2\Delta\theta(r - r_c)\,, \tag{50}$$
$$E_0^*(r) = 2\Delta\theta(r_c - r) + \sigma r\theta(r - r_c)\,, \tag{51}$$

where now the states $\bar{Q}Q$ and $\bar{Q}q\bar{q}Q$ are piecewise orthogonal. The point $r = r_c$ corresponding to degenerate states is singular. A linear combination of $\bar{Q}Q$ and $\bar{Q}q\bar{q}Q$ involves a *crossed* correlator between the channels and representing a variational improvement. The avoided crossing occurs because the finite energy of the non-diagonal $\bar{Q}Q \to \bar{M}M$ interaction lifts the degeneracy, a feature called level repulsion. The adiabatic potential curves $E_0(r)$ and $E_0^*(r)$ appear as avoided crossings on the lattice [50] with a finite and small energy repulsion and a narrow transition region of about 0.1 fm, see Fig. 5, which resemble the simple shape of Eq. (51). Therefore, as long

as the size of the system remains small, we may ignore the string breaking effect. Otherwise, one has to consider a coupled channel dynamics with $\bar{Q}Q$ and $\bar{Q}q\bar{q}Q$ states. Excited states potential curves should follow a similar pattern as Eq. (51) but with suitable modifications. Before mixing, one has the crossing among the energy levels up to $\bar{q}q$ pair creation

$$V^{(0,0)}_{\bar{Q}Q}(r) = \sigma r\,, \qquad V^{(n,m)}_{\bar{Q}q,\bar{q}Q}(r) = \Delta^{(n)}_{q\bar{Q}} + \Delta^{(m)}_{\bar{q}Q}\,, \tag{52}$$

where the double excitation character of the adiabatic potential curve is displayed explicitly and a universal string tension is assumed. The crossings must happen at $\sigma r_{\rm c}^{(n,m)} = \Delta^{(n)}_{q\bar{Q}} + \Delta^{(m)}_{\bar{q}Q}$. Avoided crossings take place when mixing among different sectors is allowed yielding energy curves sketched in Fig. 5 when using the spectrum from the RQM for $c$-hadrons [16, 17].

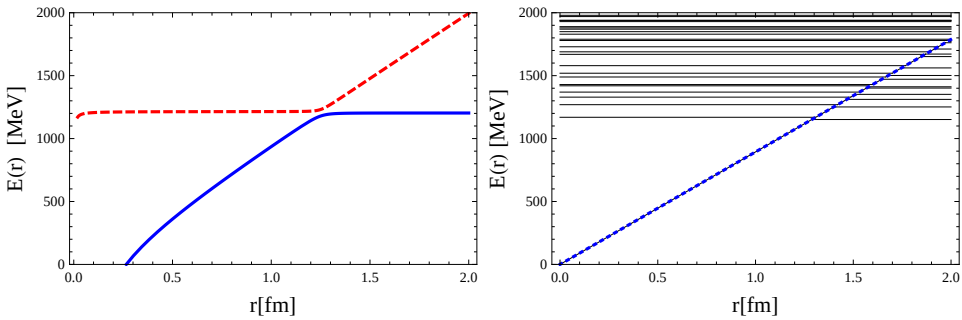


Fig. 5. Avoided crossings structure of adiabatic energy curves (in MeV) for heavy $Q\bar{Q}$ sources as a function of the distance (in fm) between the heavy sources. Left panel: Lowest states from lattice calculations with a threshold $2\Delta = 1200$ MeV added [50]. Right panel: Complete double heavy–light spectrum of the RQM for $c$-hadrons [16, 17] and included a tiny offset to make clear the structure. We also draw the envelope $\sigma r$ with $\sigma = (420\ \text{MeV})^2$.

### *4.8. Limitations in counting states*

As we have said, when the size of the system is large enough, the string breaks and the assumption of a linear potential becomes invalid, see Eq. (51). Because of the linear dependence of the size with the mass, Eq. (46), this provides a maximum mass value beyond which the RQM becomes inapplicable. A rough estimate for mesons can be made by taking $\max M_{\bar{q}q} = 2\sigma r_{\rm c}$ which for $r_{\rm c} = 1.25$ fm gives $\max M_{\bar{q}q} \sim 2.2$ GeV. For baryons, the situation is more complex. The value $\max M_{qqq} = 3\sigma r_{\rm c} \sim 3.4$ GeV is actually an upper bound for an equilateral triangular configuration, however, the string may break more economically when just *two* constituents are sufficiently far

apart, $\langle r_{ij}\rangle \sim r_c$. This corresponds to an elongated isosceles triangle (quark–diquark configuration) such that $\max M_{qqq} = 2\sigma r_c + \sigma\langle r_{12}\rangle \sim 2\sigma r_c + M_q \sim 2.5$ GeV. The RQM departs from the PDG at $M_{\bar{q}q} \sim 2$ GeV (see Fig. 4). While this poses the problem on the validity of the RQM for masses beyond the PDG saturation, it also suggests that higher mass states break up into weakly bound molecular systems with a small net contribution to the cumulative number. Actually, as argued in [52], counting hadronic states implicitly averages over some scale, and so states such as the deuteron generate fluctuations in a smaller scale[2].

For systems with a heavy quark, we have that for mesons $\Delta_{Q\bar{q}} = M_{Q\bar{q}} - m_Q = 2\sigma\langle r_{Q\bar{q}}\rangle$ and baryons $\Delta_{Qqq} = M_{Qqq} - m_Q = 2\sigma\langle r_{Qq}\rangle + \sigma\langle r_{qq}\rangle$ string breaking occurs when $\Delta_{Q\bar{q}}, \Delta_{Qqq} \sim 2\sigma r_c$.

## 5. Thermodynamics of bound states of quarks

### *5.1. The total cumulative number and equation of state in the confined phase*

The relativized quark model describes all states as bound states of $\bar{q}q$ for mesons and $qqq$ for baryons [16, 17]. The total cumulative number is then defined as

$$N(M) = N_{\bar{q}q}(M) + N_{qqq}(M)\,. \tag{53}$$

This counts the number of bound states below $M$ which is depicted in Fig. 8 (note the log scale) where a clear straight line is observed.

By quark–hadron duality, in the limit of very low temperatures, we expect to have a gas of pions (the lightest hadrons) which due to spontaneous breaking of chiral symmetry interact weakly at low energies through derivative couplings. In the chiral limit, the pions would become massless resulting in a small trace anomaly in the temperature regime where heavier hadrons are suppressed. For a gas of hadrons, the pressure reads

$$P = \sum_n \eta_n\, g_n \int \frac{d^3p}{(2\pi)^3} \log\left[1 + \eta_n e^{-\sqrt{p^2+M_n^2}/T}\right]\,, \tag{54}$$

where the sum is over *all* hadronic states including spin–isospin and antiparticle degeneracies. From here, and using the cumulative number Eq. (53)

[2] The cumulative number in a given channel in the continuum with threshold $M_{\rm th}$ is $N(M) = \sum_n \theta(M - M_n) + [\delta(M) - \delta(M_{\rm th})]/\pi$ which becomes $N(\infty) = n_B + [\delta(\infty) - \delta(M_{\rm th})]/\pi = 0$ due to Levinson's theorem. In the $NN$ channel, where $M_{\rm th} = 2M_N$ the appearance of the deuteron changes rapidly at $M = 2M_N - B_d$ by one unit so that $N(2M_N - B_d + 0^+) - N(2M_N - B_d - 0^+) = 1$, but when we increase the energy, this number decreases slowly to zero at about pion production threshold $N(2M_N + m_\pi) - N(2M_N - B_d - 0^+) \sim 0$.

obtained with the RQM [16, 17], it is straightforward to compute the trace anomaly. The comparison, shown in Fig. 2, with the continuum extrapolated results of the WB [7] and HotQCD [8] collaborations is remarkable. As a side remark, let us mention that in QCD 80% of the trace anomaly stems from the gluonic part of the operator (right-hand side of Eq. (13)) [8].

### *5.2. Polyakov loop correlators*

A straightforward consequence of Eq. (52) is that in the confined phase the correlator between Polyakov loops in the fundamental representation at large distances becomes, according to Eq. (32), with $w_0 = 1$ and $E_0(r) = \sigma r$,

$$\begin{aligned} e^{-F_1(r,T)/T} &= \left\langle \mathrm{Tr}_F \Omega(\vec{r}) \mathrm{Tr}_F \Omega(0)^\dagger \right\rangle = \sum_{n,m} e^{-V_{\bar{Q}Q}^{(n,m)}(r)/T} \\ &= e^{-\sigma r/T} + \left( \sum_n e^{-\Delta_n/T} \right)^2 , \end{aligned} \tag{55}$$

where $\Delta_n = \Delta_{\bar{q}Q}^{(n)} = \Delta_{q\bar{Q}}^{(n)}$ by charge conjugation. Then, one has

$$F_1(r,T) = -T \log \left[ e^{-V_{\bar{Q}Q}(r)/T} + e^{-F_1(\infty,T)/T} \right] , \tag{56}$$

where we have replaced $\sigma r \to V_{\bar{Q}Q}(r) = \sigma r - \pi/(12r)$. The result is depicted in Fig. 6 for $T = 50, 100, 150, 200, 250, 300$ MeV using the RQM in the case of $c$-quarks for $F_1(\infty, T)$. We see that at small temperatures there is a little change in qualitative agreement with lattice calculations [53].

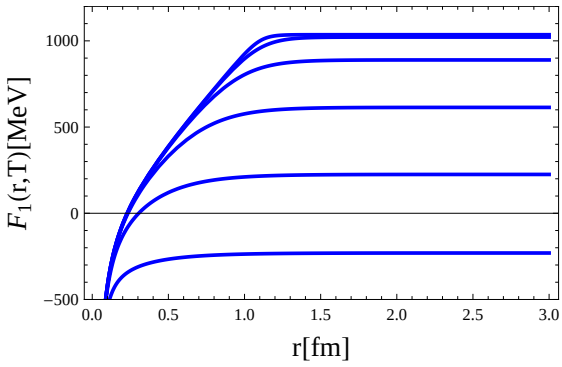


Fig. 6. Free energy $F_1(r,T)$ (in MeV) as a function of the distance for a set of increasing temperatures $T = 50, 100, 150, 200, 250, 300$ MeV (from top to bottom), using the RQM in the case of $c$-quarks. We take $\sqrt{\sigma} = 420$ MeV.

Corrections to Eq. (55) are expected, as it is based on a sharp string breaking transition and the fact that we truncated the spectrum to one light $\bar{q}q$ pair creation. The avoided crossing structure shown in Fig. 5 is modified by the finite string breaking transition region, which on the lattice and for the ground state was found to be about $\Delta r = 0.1$ fm. Moreover, for $\Delta_{\bar{q}Q} = \sigma r_{\rm c}$, we expect the $\bar{q}Q$ system to break up into $\bar{q}Q$ and $\bar{q}q$.

### *5.3. The Polyakov loop*

We can likewise consider the spectrum of a system with one heavy quark such as $c, b, t$ quarks. An equivalent cumulative number can also be defined with similar features. Because of the heavy mass, it is more convenient to subtract the heavy quark mass, $m_Q$, from the hadron mass, $M = \Delta + m_Q$. Using again the RQM for hadrons with one heavy quark, $\bar{q}Q$ for mesons and $Qqq$ for baryons [16, 17], the total cumulative number is defined as

$$N(\Delta) = N_{\bar{q}Q}(\Delta) + N_{Qqq}(\Delta)\,. \tag{57}$$

The result is depicted in Fig. 7, where similar patterns as the light quark systems are encountered, namely power behaviour for large $\Delta$ for individual $N_{\bar{q}Q}(\Delta)$ and $N_{Qqq}(\Delta)$ contributions, and Hagedorn type spectrum for the combined result, with $T_{\rm H} \sim 210$ MeV [54].

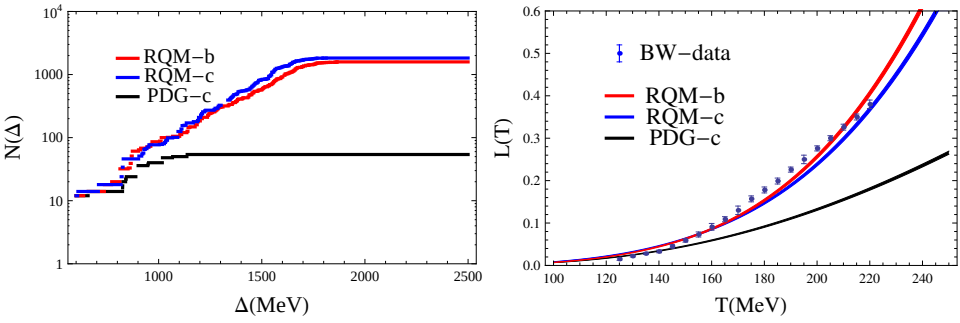


Fig. 7. Left: Cumulative number $N(\Delta)$ as a function of the $c$-quark and $b$-quark mass subtracted hadron mass $\Delta = M - m_Q$ (in MeV) with $u$, $d$ and $s$ quarks, computed in the RQM [16, 17] and from the PDG [15]. Right: Polyakov loop as a function of temperature (in MeV). Lattice data from [55] for the HISQ/tree action and [56] for the continuum extrapolated stout result. We compare lowest-lying charmed hadrons from PDG [15], the RQM spectrum with one $b$- or one $c$-quark [34].

The Polyakov loop is obtained by computing the corresponding partition function of $N_{\bar{q}Q}(\Delta)$ and $N_{Qqq}(\Delta)$ with the pertinent statistics since from Eq. (33) and Eq. (55), we get

$$L_T = \sum_n e^{-\Delta_n/T} \,. \tag{58}$$

The result can be seen in Fig. 7 and compared to lattice data from [55] for the HISQ/tree action and [56] for the continuum extrapolated stout result[3].

## 6. Limitations of the hadron resonance gas model

### *6.1. Hagedorn spectrum*

As we have mentioned, the HRG has been successfully applied in many situations below the phase transition, such as the EoS, and quark number susceptibilities, but little has been achieved with regard to understanding the emergence of hadronization in the low temperature regime. So, what is the complete hadron spectrum? Of course, we expect QCD to give the answer to this question, but this requires a knowledge of all multiparticle states of stable particles, and most of them are in the continuum. The PDG tries to answer this question by filling in the expected quark model states $\bar{q}q$ for mesons and $qqq$ for baryons. While states falling outside this category are listed as further states, whether or not the list contains redundant states is difficult to say.

In Fig. 8 we show the total cumulative number for the PDG [15] compared to the RQM [16, 17]. As can be seen, there is an exponential growth for $M \leq 2$ GeV for the PDG states [15] and $M \leq 2.5$ GeV for the RQM states [16, 17]. This remarkable feature of the cumulative number, first noted by Hagedorn [57], has fascinated theoreticians for decades. The exponential growth is of the form $N(M) \sim e^{M/T_{\rm H}}$, where $T_{\rm H}$ is the so-called Hagedorn temperature. This pattern was predicted with very few states and an ever increasing exponential spectrum was anticipated as new states entered the hadronic list. Different upgrading analyses have confirmed this exponential growth [58, 59] and even two different Hagedorn temperatures have been reported (see, however, the discussion around Fig. 4). The onset of the Hagedorn spectrum has been questioned more recently [60]. The growth happens at about $M \sim 1.5$ GeV and continues with the *same* slope until $M \sim 2.1$ GeV. The pattern is even more clear in the RQM, where the trend stretches up to $M \sim 2.5$ GeV. The consequence of a truly Hagedorn

[3] We are cavalier on the renormalization issues and multiplicative ambiguities in $L_T$. Further details are discussed in Ref. [34].

temperature is that the partition function, and hence all thermodynamics quantities develop a pole at the Hagedorn temperature

$$\mathcal{A}_{\rm HRG} \to \frac{A}{T - T_{\rm H}} \,. \tag{59}$$

This form is not observed on the lattice although good fits in the range of 50 MeV $< T <$ 180 MeV for the trace anomaly yield a value of about $T_{\rm H} \sim 220$ MeV.

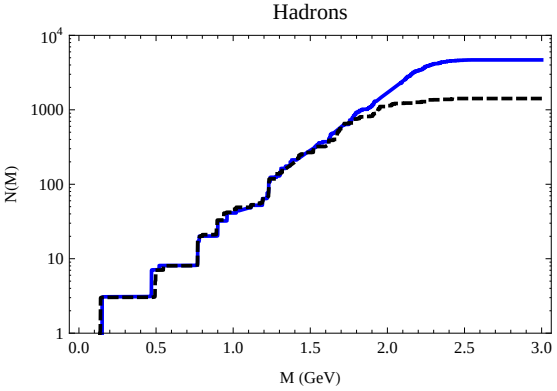


Fig. 8. Cumulative number for the PDG [15] (dashed) and the RQM [16, 17] (full).

One important consequence of such a favourable comparison between PDG and RQM is that it may provide a clue to the onset of the Hagedorn spectrum. We can estimate the asymptotic behaviour for both $\bar{q}q$ and $qqq$ spectra in the RQM as the model Hamiltonian is known. As we have shown, we expect a power behaviour for both $N_{\bar{q}q}(M)$ and $N_{qqq}(M)$, a fact confirmed in Fig. 4 where the separated contributions in a log–log scale exhibit this power-like behaviour. The question is how is it possible that summing two polynomials we end up with an exponential?

Using the MIT bag model [61] this question was answered by Kapusta [62] since then the cumulative number can be computed as $\sum_n N_n(M)/n!g^n$ from Eq. (43) by using a constant bag volume and evaluating the phase-space integral for free particles. We have checked this explicitly by summing the bag modes [37].

### *6.2. Finite width corrections*

Of course, the discrete summation involved in the cumulative number definition requires considering all masses of states to be interpreted as bound states. In reality, most of the states listed in the PDG are resonances, *i.e.* unstable particles which have instead a mass spectrum characterized by a distribution $\rho(\mu)$ which is peaked at $\mu = M_n$ with a certain width $\Gamma_n$.

This idea has been implemented by the half-width rule, where resonance masses are regarded as random variables with an uncertainty of half the width [63]. This interpretation has been fruitful in describing the Regge spectrum of mesons [64, 65], hadronic form factors [66] as well as providing an error estimate for the cumulative number itself [22]. This also provides a quantitative way of defining a figure of merit for the quark model taking the width as a genuine uncertainty.

In a quantum mechanical picture, where the resonance decay can be viewed as a tunneling process, the mass shift of a unstable state is negative as the infinite barrier becomes finite making the energy shift negative. As a consequence, the cumulative number would increase for a fixed mass, $N_{\text{resonance}}(M) > N_{\text{bound}}(M)$. This effect goes in the opposite direction of making $N_{\text{RQM}}(M)$ and $N_{\text{PDG}}(M)$ to agree in the upper part of the spectrum, and that the outnumbering of $\bar{q}q$ and $qqq$ states in the RQM would be a genuine one.

### *6.3. Excluded volume condition*

The reason for the failure of the HRG in describing the trace anomaly at $T \sim 170$ MeV may be sought by questioning any of the assumptions involved. One of them, the finite size of hadrons may be tested by computing the excluded volume.

In an ideal world where the hadrons live forever they still have a finite size. This is the case, for instance, in the large $N_c$ limit, where one has $\Gamma/M = \mathcal{O}(N_c^{-1})$ but their size is $r = \mathcal{O}(N_c^0)$. Due to the finite hadronic size, when hadrons overlap their underlying composite nature becomes relevant, particularly regarding the Pauli principle as applied to the constituent quarks.

The finite volume corrections have often been addressed along the lines of statistical mechanics for real gasses where hadron volumes are usually assumed to be similar (see *e.g.* [21]). Taking into account how these corrections originate in the quantum virial expansion as repulsive contributions through negative phase shifts, it is unclear what are the actual values one should take for the volume without actually carrying the phase shift analysis. In a bound states picture, which is the spirit of the HRG since finite width effects are disregarded, the size of the bound state is expected to increase with the mass of the state.

One simple estimate of the size of the hadron can be made by using the MIT bag model [61], where the volume $V_i$ of the hadron is a natural concept since in that model hadrons with a mass $M_i$ have a sharp edge, $r_i$, where

$$V_i = \frac{4\pi}{3} r_i^3 = M_i/(4B)\,, \qquad B = (0.166\ \text{GeV})^4\,, \tag{60}$$

and thus the volume grows with the mass.

In the case of the RQM where particles are interacting through a confining $\sigma r_{ij}$ potential, and hadrons are localized but have a diffuse edge, the volume is not a well defined concept. To estimate the value of the volume occupied by the hadron in the RQM, we take as the meson radius $\langle r_{\bar{q}q}\rangle/2$ and for the baryon the radius of the equilateral triangle $\langle r_{qq}\rangle/\sqrt{3}$. This yields the volume estimate

$$V_i = \frac{4\pi}{3}\frac{M_i^3 c_i^3}{\sigma^3}\,, \qquad \sqrt{\sigma} = 0.42\ \text{GeV}\,, \tag{61}$$

where $c_i = 1/4$ for mesons and $c_i = 1/(3\sqrt{3})$ for baryons. With this prescription, baryons occupy a smaller volume for the same mass. These are crude estimates, which assume a sharp edge of the hadron, but they show that the volume does depend on the mass.

Rather than trying to model finite volume corrections, we will analyze the quite natural condition that the excluded volume cannot be negative, or equivalently that the occupied volume is smaller than the total volume. This means

$$\sum_i V_i N_i \le V\,, \qquad \sum_i V_i \int \frac{d^3p}{(2\pi)^3}\frac{g_i}{e^{E_i(p)/T}\pm 1} \le 1\,. \tag{62}$$

In Fig. 9, we illustrate the situation by depicting the occupied volume condition using the MIT bag model volume, Eq. (60), and our estimate for the RQM hadronic volume, Eq. (61), using both the RQM spectrum and the

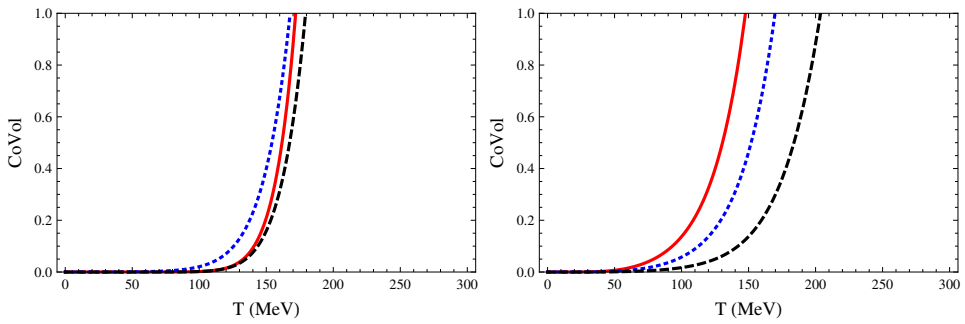


Fig. 9. The occupied volume condition using three different models for the relation between the volume and the mass for a hadron. The upper edge of the figure expresses the maximum limit beyond which the conditions is violated. We show: (left panel) RQM spectrum with $V_i \sim M_i^3$ (dotted), PDG spectrum with $V_i = M_i/(4B)$ (full), PDG spectrum with $V_i = M_i^3$ (dashed); (right panel) PDG spectrum with constant volume using $r = 1$ fm (full), $r = 0.75$ fm (dotted) and $r = 0.5$ fm (dashed).

PDG spectrum. As one can see, the condition is violated for temperatures $T \sim 150$–$180$ MeV where the HRG departs from the lattice data. This is an interesting fact, since it relates the crossover to a volume effect, which deserves further investigation. For comparison, we also show in the right panel the results for a constant hadronic volume taking the radius values $r = 0.5, 0.75, 1$ fm. The choice $r \sim 0.75$ fm resembles the RQM and bag excluded volume condition.

## 7. Insights from gluodynamics

Matters get simpler in the case of pure gauge theories where gluons are the only degrees of freedom. In QCD, this corresponds to taking the limit $m_q \to \infty$ for *all* quark species. As mentioned, the Polyakov loop in the *fundamental* representation becomes a true order parameter of the deconfinement phase transition since at low temperatures it vanishes as $L_T = \mathcal{O}(e^{-m_q/T})$ in this limit. The Polyakov loop in the *adjoint* representation does not vanish below $T_c$. Gluon–glueball duality means in this case that *any* observable defined as an expectation value of a gauge invariant and hence colour singlet operator can be determined in terms of purely colour singlet states in the confined phase. As we will illustrate, this means in practice that the EoS can be determined in terms of glueballs (bound states of gluons) whereas the Polyakov loop in the adjoint representation can be determined from gluelumps which are bound states of gluons in the presence of a colour octet source [67–70].

### *7.1. The glueball gas model*

In pure gauge theories, the glueball spectrum has been determined in the lattice [71]. (For full unquenched QCD glueball studies see *e.g.* [72]. A general perspective including phenomenology has been reviewed in Ref. [73].)

Gluons are massless particles for which the helicity formalism [74] is the proper one. For spin-1 particles, this means that just the $\pm 1$ projections are possible. This issue was first discussed by Barnes [75] within the context of gluonium (see [76–78] for an upgraded discussion). In the helicity formalism, two-gluon states $J^{\rm PC} = 1^{-+}, 1^{++}, 3^{-+}, 5^{-+}$ are forbidden in accordance to lattice results [71, 79]. The glueball spectrum of two gluons might be obtained from a full fledged solution of the Bethe–Salpeter equation for two spin-1 particles [80–83]. In practice, solving these equations requires an ansatz for the kernel which is usually obtained by making reasonable approximations. For our discussion, we will make some drastic approximations which actually illustrate one important point regarding gluon–glueball duality at finite temperature. We will assume the following rotational invariant

and spin independent Hamiltonian in the CM system

$$H\psi_n = \left(2p + \sigma_A r - \frac{3\alpha_{\rm s}}{r}\right)\psi_n = M_n\psi_n\,. \tag{63}$$

In this scheme, the total spin of the glueball $J$ is obtained by composing the gluons spin and the relative orbital angular momentum. Due to Bose statistics, the total glueball wave function must be, besides a colour singlet state, fully symmetric. Thus, the spin and orbital part must be both either symmetric or antisymmetric. This gives a total degeneracy of $(2l+1)g(g\pm 1)/2$ for even/odd $l$, where $g$ is the number of spin states of the gluon. The lowest one is the $0^{++}$ glueball [43]. Then, the cumulative number becomes

$$N(M) = \sum_{n,l} \nu_l (2l+1)\theta(M - M_{nl})\,, \tag{64}$$

where $\nu_l = g(g\pm 1)/2$ for even/odd $l$.

A simple estimate using the uncertainty principle for the ground state is made by taking $pr \sim 1$, thus

$$M_0 = \min\left[\frac{2}{r} + \sigma_A r - \frac{3\alpha_{\rm s}}{r}\right] = 2\sqrt{(2-3\alpha_{\rm s})\sigma_A} \approx 4\sqrt{\sigma}\,.$$

For excited states, an estimate can be obtained by using the Bohr–Sommerfeld quantization condition (WKB spectrum). For $s$-wave, this gives

$$2\int_0^a dr\, p(r) = 2\pi(n+\alpha)\,,$$

where $p(r) = (M - \sigma_A r + 3\alpha_{\rm s}/r)/2$, $a$ is the classical turning point, $p(a) = 0$, and $\alpha$ depends on the boundary conditions. This produces (neglecting the Coulomb term)

$$M_n^2 = 4\pi\sigma_A(n+\alpha) \qquad \text{(WKB, } s\text{-wave)}\,.$$

More systematically, the eigenvalues of the CM Hamiltonian, Eq. (63), can be computed by diagonalizing it in the harmonic oscillator wave functions basis

$$R_{nl}(r) = \frac{u_{nl}(r)}{r} = \frac{e^{-\frac{r^2}{2b^2}}}{\sqrt[4]{\pi}}\left(\frac{r}{b}\right)^l \sqrt{\frac{(n-1)!2^{l+n+1}}{b^3(2l+2(n-1)+1)!!}} L_{n-1}^{l+\frac{1}{2}}\left(\frac{r^2}{b^2}\right)\,, \tag{65}$$

where $L_{n-1}^{l+\frac{1}{2}}(x)$ are associated Laguerre polynomials. The advantage of the harmonic oscillator basis is that the matrix elements of the pseudodifferential operator $|\vec{p}|$ are simply related to those of $r$ [4].

The reduced wave functions $u_{nl}(r)$ are normalized to unity

$$\int_0^\infty dr r^2 R_{nl}(r)^2 = \int_0^\infty dr u_{nl}(r)^2 = 1\,,$$

and satisfy the equation

$$-u''_{nl}(r) + \left[\frac{r^2}{b^4} + \frac{l(l+1)}{r^2}\right] u_{nl}(r) = \frac{1}{b^2}(2l+4n-1)u_{nl}(r)\,. \tag{66}$$

Here, $b$ has dimensions of length. The single-particle energies are

$$\epsilon_{nl} = \frac{1}{2Mb^2}\,(4n+2l-1) = \omega\,(2n+l-1/2)\,,$$

where the oscillator frequency is $\omega = 1/(Mb^2)$. Thus, we can compute the matrix elements $H_{nl,n'l}$ up to some maximum values of $n$ and $l$ and diagonalize the truncated Hamiltonian. A list of eigenvalues (for a linear potential) for $n \leq 8$ and $l \leq 13$ can be looked up in Ref. [84]. The quoted accuracy is right provided we take the dimension as large as $N = 100$.

A derivative expansion [85] can be used to evaluate the cumulative number of the Hamiltonian in Eq. (63). In the present context, this is closely related to a semiclassical expansion and a large mass expansion. A direct application of the results in [85] gives[5]

$$\begin{aligned} N_{2g}(M) &= \frac{g^2}{2}\int \frac{d^3x d^3p}{(2\pi)^3}\theta(M - H(p,r)) + \ldots \\ &= \frac{g^2}{2}\left(\frac{M^6}{720\pi\sigma_A^3} + \frac{\alpha_{\rm s}M^4}{16\pi\sigma_A^2} + \frac{9\alpha_{\rm s}^2M^2}{8\pi\sigma_A} - \frac{M^2}{9\pi\sigma_A} + \ldots\right)\,. \end{aligned} \tag{67}$$

By restoring the $\hbar$s in the Hamiltonian, $\sigma_A \to \sigma_A/\hbar$ and $\alpha_{\rm s} \to \hbar\alpha_{\rm s}$, we can see that the first quantum corrections enter in the last term quoted. As advertised, the derivative expansion corresponds to a power expansion in $M$, with a general form

$$N(M) = \sum_n a_n M^n\,. \tag{68}$$

[4] Beware that the Fourier–Bessel transform introduces an additional phase $(-1)^n$ to the momentum space wave function $P_{nl}(p) \equiv \int_0^\infty j_l(pr)R_{nl}(r)r^2dr = (-1)^n R_{nl}(r = pb^2)$.

[5] For simplicity, here we disregard the effect of the different degeneracies in even and odd partial waves. It has no effect at leading order in $\hbar$.

We show in Fig. 10 the comparison of the full diagonalization in the harmonic oscillator basis to the semiclassical large mass expansion. As we see, the agreement is rather good for a relatively low value of $N(M)$.

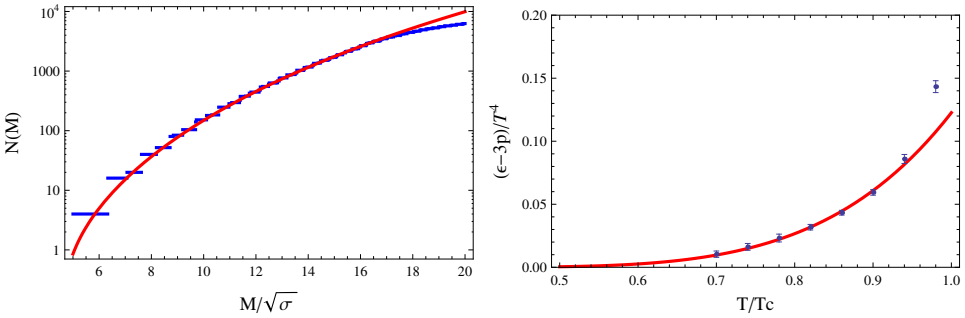


Fig. 10. Left panel: Cumulative number of states for two-gluon glueballs as a function of the mass in units of the fundamental string tension $\sqrt{\sigma}$, compared to the semiclassical approximation. Right panel: Two-gluon states contribution to the trace anomaly compared to the lattice data from the WB Collaboration [40].

It is now straightforward to compute the corresponding contribution to the trace anomaly from the expression[6]

$$\mathcal{A}^{2g}_{\text{glueball}}(T) = \sum_n \sum_{k=1}^{\infty} \frac{1}{2\pi^2 k} \left(\frac{M_n}{T}\right)^3 K_1\left(\frac{kM_n}{T}\right) , \tag{69}$$

where $M_n$ are eigenvalues of $H$ with the corresponding spin–orbit-colour degeneracies compatible with the colour singlet and Bose character of the two-gluon states. The most recent lattice data from the WB Collaboration [40] include 7 points for $\mathcal{A}(T)$ below $T_c$ which being a dimensionless quantity depends just on the dimensionless ratio $T/T_c$. In our case, we only have the dimension $\sqrt{\sigma}$ and thus the dimensionless $\mathcal{A}_{2g}(T)$ depends on $T/\sqrt{\sigma}$. Thus, we can determine $T_c/\sqrt{\sigma}$ from a fit of $\mathcal{A}_{2g}(T)$ to the lattice data [40].

For $g=3$, we get $\chi^2 = 3.2$ for the first 6 lattice data but $\chi^2/\nu = 56/(7-1)$ when the last point is added. Actually, the value of $\sigma$ is already determined by the first point, although its error decreases as new points are included in the fit. This provides some robustness to the analysis, and indicates that for $T \le 0.9 T_c$ the trace anomaly is mainly saturated by two-gluon glueballs. The fit gives

$$\frac{T_c}{\sqrt{\sigma}} = 0.71247\,, \qquad \text{lattice} \quad 0.629(3)\,, \tag{70}$$

a quite reasonable result.

[6] This expression follows from the expansion of Eq. (1) in powers of $e^{-E_n(p)/T}$ prior to integrate over the momentum.

We can proceed further in the analysis by rewriting the trace anomaly for bosons as

$$\mathcal{A}(T) \;=\; \sum_{k=1}^{\infty} \int dM \frac{\partial N(M)}{\partial M} \frac{1}{2\pi^2 k} \left(\frac{M}{T}\right)^3 K_1\left(\frac{kM}{T}\right) ,$$

and making use of the formula

$$\int_0^{\infty} dM \left(\frac{M}{T}\right)^3 \frac{M^{n-1}}{2\pi^2 k} K_1(kM/T) = \frac{(n+2)(2T)^n \Gamma\left(\frac{n}{2}+1\right)^2}{2\pi^2 k^{n+4}} , \qquad (71)$$

as well as the large $M$ expansion of the cumulative number, Eq. (68). Then, we get an equivalent large $T$ expansion for the trace anomaly

$$\mathcal{A}(T) = \sum_n a_n \frac{n(n+2)}{2\pi^2} (2T)^n \zeta(n+4) \Gamma\left(\frac{n}{2}+1\right)^2 . \qquad (72)$$

For instance, in the two-gluon sector, we get

$$\mathcal{A}_{2g}(T) = \frac{2048\pi^8}{3465} a_6 T^6 + \frac{128\pi^6}{1575} a_4 T^4 + \frac{128\pi^6}{1575} a_2 T^2 . \qquad (73)$$

Applying the results in Ref. [85] for the coefficients $a_i$ yields

$$\mathcal{A}(T) = \frac{32768\,\pi^7 T^6}{113669325\,\sigma^3} + \frac{512\,\pi^5 \alpha_s T^4}{127575\,\sigma^2} + \frac{16}{945}\pi^4 T^2 \left(\frac{2\alpha_s^2}{\pi\sigma} - \frac{16}{81\pi\sigma}\right) . \qquad (74)$$

The interesting feature is that the effect of the full quantized spectrum can be very well described by the semiclassical expansion for the temperatures available on the lattice. Thus, we can use instead the semiclassical expansion to fit the parameters and sidestep the diagonalization.

As a further remark, let us note that a direct attempt to fit the polynomial formula fails since there are too few data points and the curve is smooth. The correlations implicit in the $2g$-Hamiltonian among the different coefficients are however enough to guide the fit. The last data point is intriguing and the most obvious candidate to fill the gap is by looking at three-gluon glueballs. The three-gluon potential on the lattice has been analyzed [86] and it has been found that the triangle is preferred to the starfish configuration. In a semirelativistic framework, three-gluon glueballs have been addressed in Ref. [87]. Thus, we can take the partonic Hamiltonian result which sets a scale separation between $2g$-WKB and $3g$ glueballs

$$\mathcal{A}_{3g}(T) \sim e^{-M_{3g}/T} \ll \mathcal{A}_{2g}(T) . \qquad (75)$$

Whether or not $3g$ saturate the missing contribution, or even multigluonic states are needed remains to be seen. On the other hand, let us note that using the lowest glueballs on the lattice we found [88] that while the cumulative number could, after come coarse graining, be described as exponentially growing with $T_{\rm H} = 2.8T_{\rm c}$, the effect on the trace anomaly was tiny. The High-Precision Thermodynamics in connection to the Hagedorn Density of States has been discussed in [89]. A satisfactory fit with $T_{\rm H} = 1.024(3)T_{\rm c}$ was obtained by adding a string motivated Hagedorn spectrum to the lowest $0^{++}$ and $2^{++}$ glueballs (see also [90] and [40] ). The fate of glueballs above the phase transition has been analyzed in Ref. [91].

### *7.2. The adjoint Polyakov loop and the gluelump spectrum*

According to duality, the adjoint Polyakov loop can be computed in the confined phase in terms of the gluelump spectrum. In the simplest case, this system corresponds to one massless spin-1 particle and one gluon source (infinitely heavy) which is the CM system. The Salpeter equation for the Hamiltonian operator (the Coulomb term is omitted) reads

$$H\psi_n = (p + \sigma_A r)\psi_n = M_n \psi_n \,, \tag{76}$$

which by rescaling the coordinate can be brought to the glueball spectrum

$$M_{\rm gluelump} = M_{\rm glueball}/\sqrt{2} \,. \tag{77}$$

Thus, the smallest mass gap in the pure gauge theory is the gluelump and not the glueball! This scaling relation of the spectrum implies that the partition function fulfills $Z_{\rm gluelumps}(T) = (2/g) Z_{\rm glueballs}(T/\sqrt{2})$. Likewise, for the adjoint Polyakov loop at low temperatures implies

$$\langle \Omega_8 \rangle_T \sim Z_{\rm gluelumps}(T) = \sum_n e^{-\Delta_n/T} \neq 0 \qquad (T < T_{\rm c}) \,. \tag{78}$$

### *7.3. The powers of deconfinement*

One straightforward application of the glueball gas is that because they are heavy, the pressure in the confined phase is tiny,

$$P(T) = P_{\rm glueball}(T) \approx e^{-M_G/T} \qquad (T < T_{\rm c}) \,, \tag{79}$$

where $M_G \gg T_{\rm c}$. On the other hand, at high temperatures the pressure is due to a free gluon gas

$$P_{\rm gluons}(T) = \frac{b_0}{2} T^4, \qquad b_0 = \frac{2\pi^2}{45}\left(N_c^2 - 1\right) \qquad (T \gg T_{\rm c}) \,. \tag{80}$$

When the trace anomaly for gluodynamics was first evaluated on the lattice [26] across the phase transition, the common wisdom was the standard textbook explanation of the deconfinement based on the MIT bag model, where hadrons are bubbles in the strongly interacting vacuum with an energy density $B \sim M_H/V \sim 1\ \mathrm{GeV/fm}^3 \sim (0.3\ \mathrm{GeV})^4$ [61]. Thus, the total pressure was

$$P(T) = P_{\mathrm{gluons}}(T) - B\,, \qquad T > T_{\mathrm{c}}\,, \tag{81}$$

and continuity of the pressure implies $P_{\mathrm{gluons}}(T_{\mathrm{c}}) = B$ for $M_G \gg T_{\mathrm{c}}$, and thus yields the trace anomaly

$$\mathcal{A} = \frac{\epsilon - 3P}{T^4} = \frac{4B}{T^4}\,, \qquad T > T_{\mathrm{c}}\,. \tag{82}$$

However, this behaviour is in complete disagreement with the old [26] and newest [40] lattice data.

Ten years ago, we looked into the Polyakov loop and found that, contrary to expectations, one has inverse temperature power corrections above the phase transition of the form of Eq. (24) [31], with a remarkable good description of the data in a wide range of temperatures. These power corrections were quite surprising and completely unexpected[7], since it indicated the breakdown of perturbation theory for temperatures as large as $5T_{\mathrm{c}}$, but have been verified on the lattice [35, 36] and other models [93].

One possibility to explain the trace anomaly data is to assume instead that there is a temperature dependence in the bag constant (a fuzzy bag [94], see also [88, 95–97] for a unified setup)

$$P(T) = P_{\mathrm{gluons}}(T) - B_{\mathrm{fuzzy}}(T) \quad (T > T_{\mathrm{c}})\,, \qquad P(T_{\mathrm{c}}) = P_{\mathrm{glueballs}}(T_{\mathrm{c}}) = 0\,. \tag{83}$$

An inspiring consequence from the power corrections of Eq. (24) is to assume

$$B_{\mathrm{fuzzy}} = \frac{b_0}{2} T_{\mathrm{c}}^2 T^2 \qquad \longrightarrow \qquad P = \frac{b_0}{2}\left(T^4 - T^2 T_{\mathrm{c}}^2\right)\,, \tag{84}$$

which gives

$$\mathcal{A} = \frac{\epsilon - 3P}{T^4} = b_0 \left(\frac{T_{\mathrm{c}}}{T}\right)^2\,, \qquad b_0 = 3.51\,. \tag{85}$$

The result is presented in Fig. 11 and compared with the most recent lattice data from the WB Collaboration [40]. As we see, the agreement for $T > 1.5\,T_{\mathrm{c}}$ of such a simple model is impressive. These features are confirmed

[7] In fact, a $1/T^2$ behaviour in the trace anomaly data of [26] was already noted by the authors of [92].

for any $N_c$ [98, 99]. Further analyses involve renormalization group resumations [88], hard thermal loops [100] as well as holographic methods [101–103], but a clear physical picture of the undoubtful but mysterious powers is still lacking.

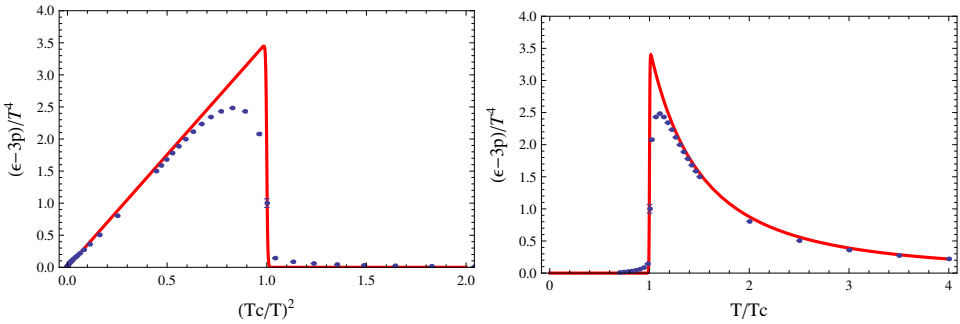


Fig. 11. Trace anomaly as a function of $1/T^2$ and $T$ comparing the fuzzy bag of Pisarski [94] $\mathcal{A}(T) = \frac{(N_c^2-1)\pi^2}{45}\left(\frac{T_c}{T}\right)^2\theta(T-T_c)$ with the lattice data from the WB Collaboration [40].

## 8. Emergence of duality with Polyakov loop models

### *8.1. Chiral quark models at finite temperature*

Up to now, we have assumed that duality holds without specifying how this might occur from a microscopic point of view. Here, we want to illustrate how duality arises from quark models and the relevant provisos to achieve this goal. A full QCD argument for the hadronization of the Polyakov loop was advanced and elaborated in Refs. [34, 37].

Chiral quark models have been used (*e.g.* [104] and references therein) for a long time to describe the chiral phase transition. It was then realized that they lead to a wrong $N_c$ counting of thermal corrections, since they are described as one quark loop and hence are $\mathcal{O}(N_c)$. In reality, they correspond to zero point energy of meson states which are $\mathcal{O}(N_c^0)$. For instance, in the quark condensate, one has $\langle\bar{q}q\rangle_0 = \mathcal{O}(N_c)$ but $\langle\bar{q}q\rangle_T - \langle\bar{q}q\rangle_0 = \mathcal{O}(N_c^0)$ (wrongly counted by the CQM as $\mathcal{O}(N_c)$). This observation was well known although surprisingly nothing was done about it. The requirement of large gauge invariance motivated us for the introduction of the Polyakov line as an independent variable [105] which has a local and quantum character. Previous works had already dealt with this coupling [106, 107] initiating the Polyakov–Nambu–Jona-Lasinio (PNJL) saga [108–117] where the Polyakov line has been taken global and classical. This allowed to study the interplay between chiral symmetry restoration and breakdown of the

center symmetry although, as we have repeatedly pointed out in our previous works [105, 118–121], this generates an undesirable ambiguity of group coordinates as well as a non-vanishing value for the Polyakov loop in the adjoint-representation, contradicting lattice simulations[8]. These difficulties may be overcome [105, 118] by recognizing the local and quantum nature of the Polyakov loop. Using this interpretation, we have shown that a gateway to the hadron resonance gas may be established if the motion of quarks in the field generated by the Polyakov loop is quantized.

We note that on the lattice [124], the HRG has been deduced in strong coupling and for large $N_c$ by considering hadrons at rest.

### *8.2. The quantum and local Polyakov loop*

As we have mentioned above, large gauge invariance is an important restriction at finite temperature which breaks down in perturbation theory. In the Polyakov gauge, one can automatically implement large gauge invariance by considering the Polyakov loop line $\Omega(\vec{x})$ as an independent variable, which in the Polyakov gauge becomes a diagonal unitary matrix in colour space. This is equivalent to a minimal coupling scheme in the time derivative of a dynamical quark or gluon field. We refer to Refs. [105, 118–120] for further motivation.

Following this prescription, the partition function of the Chiral Quark Model (CQM) at finite temperature can be written as

$$Z_{\mathrm{CQM}} = \int D\Omega\, e^{-S(T,\Omega)}\,, \tag{86}$$

where $\Omega = e^{igA_0/T}$ and $D\Omega$ is the invariant SU($N_c$) Haar group integration measure, for each SU($N_c$) variable $\Omega(\vec{x})$ at each point $\vec{x}$. Here, the action is

$$S(T,\Omega) = S_q(T,\Omega) + S_G(T,\Omega)\,. \tag{87}$$

The fermionic contribution depends on the quarks (and antiquarks), and it is obtained from the corresponding fermion determinant. Assuming mass-degenerated quarks, for simplicity, the effective action reads

$$S_q(T,\Omega) = -2\sum_q \int \frac{d^3x d^3p}{(2\pi)^3} \left(\mathrm{Tr}_c \log\left[1+\Omega(\vec{x})\, e^{-E_q(p)/T}\right] + \mathrm{c.c.}\right)\,, \tag{88}$$

where c.c. stands for the complex conjugated contribution stemming from the antiquarks and 2 is the spin degeneracy factor for spin 1/2 particles. Here, $E_q(p) = \sqrt{\vec{p}^{\,2} + M_q^2}$ is the energy of a quark with total mass $M_q =$

[8] See Refs. [122, 123] for a study of this interplay from effective potential methods.

$M_0 + m_q$, and $M_0$ is the constituent mass. As one can see, the diagonal part of the Polyakov loop corresponds to consider chemical potentials for different colour species. Large colour gauge invariance is implemented by just averaging over group elements. We will check whether this minimal coupling scheme for the Polyakov line complies with known QCD properties [34, 37], such as the fact that the expectation value of the Polyakov loop admits a hadronic representation.

### *8.3. Hadronic representation of the Polyakov loop*

In order to see this, consider a system with $N_f$ dynamical quarks and an extra heavy quark (not antiquark) of an arbitrarily large mass $m_H$ at rest located at a fixed point and with fixed spin and colour $a = 1, \ldots, N_c$. From Eq. (88), the change in the effective action is

$$S_q\,(N_f+1) - S_q(N_f) = -2\log\left(1 + \Omega_{aa} e^{-E_h/T}\right) \approx -2e^{-m_H/T}\Omega_{aa}\,, \quad (89)$$

yielding the partition function

$$\begin{aligned}\frac{Z^{\rm H}_{\rm CQM}(N_f+1)}{Z_{\rm CQM}(N_f)} &= 1 + \langle\Omega_{aa}\rangle 2e^{-m_H/T} + \ldots \\ &= 1 + \frac{1}{N_c}\langle {\rm Tr}_c\Omega\rangle 2e^{-m_H/T} + \ldots \end{aligned} \quad (90)$$

after averaging over colour degrees of freedom implied by $D\Omega$. Thus, we get

$$\frac{1}{N_c}\langle {\rm Tr}_c\Omega\rangle = \lim_{m_H\to\infty}\frac{1}{2}\left[\frac{Z^{\rm H}_{\rm CQM}(N_f+1)}{Z_{\rm CQM}(N_f)} - 1\right] e^{m_H/T}\,. \quad (91)$$

To evaluate the r.h.s., we explicitly separate in the corresponding HRG hadrons composed of hadrons made of $N_f$ dynamical quarks and one extra heavy quark. The mass of such hadrons can be written as

$$M_{q\ldots,H} = \Delta_{q\ldots} + m_H\,, \quad (92)$$

where by definition in $\Delta$, it has been subtracted the mass of the heavy quark. On the other hand, the HRG partition function with $N_f+1$-flavours with this extra heavy quark $H$ can be separated into hadrons containing it or not. To do this, we reinstate the finite box quantization conditions on the momentum $\vec{p}$ to make sense of the limit $m_H \to \infty$ and $V \to \infty$ (the Compton wavelength of the heavy quark is shorter than the box size) and get

$$\log Z^H_{\rm HRG}(N_f+1) = \log Z_{\rm HRG}(N_f) + \sum_{\vec{p},\alpha}\eta_\alpha g_\alpha \log\left[1 + \eta_\alpha e^{-(\Delta_\alpha + m_H)/T}\right]\,. \quad (93)$$

In the limit $m_H \to \infty$, only the states with $\vec{p} = 0$ survive corresponding to a heavy Hadron at rest contribution, and thus we get the result

$$\frac{1}{2}\sum_\alpha g_\alpha e^{-\Delta_\alpha/T} = \lim_{m_H\to\infty}\frac{1}{2}\left[\frac{Z^{\rm H}_{\rm HRG}(N_f+1)}{Z_{\rm HRG}(N_f)} - 1\right] e^{m_H/T}\,. \tag{94}$$

Quark–hadron duality at this level implies $Z_{\rm HRG} = Z_{\rm CQM}$, so that we get

$$\frac{1}{N_c}\langle {\rm Tr}_c \Omega\rangle = \frac{1}{2}\sum_\alpha g_\alpha e^{-\Delta_\alpha/T} \tag{95}$$

providing confidence on the assumed minimal coupling of the Polyakov line to quarks.

### *8.4. From chiral quark models to the hadron resonance gas*

The previous models can be pictured as multiquark states which are created or annihilated at point $\vec{x}$ and momentum $\vec{p}$ with factors $\Omega(\vec{x})e^{-E_p/T}$ and $\Omega(\vec{x})^\dagger e^{-E_p/T}$. This corresponds to classical particles with internal quantum numbers and statistic, *i.e.* to a second quantized but not first quantized formalism.

At low temperatures, quark Boltzmann factors are small $e^{-E_p/T} \ll 1$, and the quark contribution to the action becomes small

$$S_q[\Omega] = -2N_f \int \frac{d^3x d^3p}{(2\pi)^3}\left[{\rm Tr}_c\Omega(x) + {\rm Tr}_c\Omega^\dagger(x)\right] e^{-E_p/T} + \dots \tag{96}$$

Thus, one has

$$\begin{aligned} Z_{\rm CQM} &= \int D\Omega\, e^{-(S_q[\Omega]+S_G[\Omega])} = \left\langle e^{-S_q[\Omega]}\right\rangle_G \\ &= \left\langle 1 - S_q[\Omega] + \tfrac{1}{2}S_q[\Omega]^2 + \dots\right\rangle_G\,, \end{aligned} \tag{97}$$

where $\langle\,\rangle_G$ incorporates besides the group integration measure a gluon piece which needs not be specified at this point. This expansion corresponds to a partonic expansion in terms of constituents $q, \bar{q}, \bar{q}q, \dots$ The lowest non-vanishing $\bar{q}q$ contribution reads

$$\begin{aligned} Z_{\bar{q}q} &= (2N_f)^2 \int \frac{d^3x_1 d^3p_1}{(2\pi)^3}\int \frac{d^3x_2 d^3p_2}{(2\pi)^3} e^{-E_1/T} e^{-E_2/T} \underbrace{\left\langle {\rm Tr}_c\Omega(\vec{x}_1){\rm Tr}_c\Omega^\dagger(\vec{x}_2)\right\rangle_G}_{e^{-\sigma|\vec{x}_1-\vec{x}_2|/T}} \\ &= (2N_f)^2 \int \frac{d^3x_1 d^3p_1}{(2\pi)^3}\frac{d^3x_2 d^3p_2}{(2\pi)^3} e^{-H(x_1,p_1;x_2,p_2)/T}\,, \end{aligned} \tag{98}$$

where the $\bar{q}q$ Hamiltonian reads

$$H(x_1,p_1;x_2,p_2) = E_1 + E_2 + V_{12}\,. \tag{99}$$

Note that in the CM frame, we get the same Salpeter equation we discussed previously. Quantization in the CM frame $p_1 = -p_2 \equiv p$ leads to

$$\left(2\sqrt{p^2+M^2} + V_{q\bar{q}}(r)\right)\psi_n = M_n\psi_n\,, \tag{100}$$

and boosting the CM to any frame with momentum $P$, we get the result

$$Z_{\bar{q}q} \to \sum_n \int \frac{d^3R d^3P}{(2\pi)^3} e^{-\frac{\sqrt{M_n^2+P^2}}{T}}\,, \tag{101}$$

which corresponds to the lowest order in a gas of non-interacting mesons [125]. We have checked that this equivalence holds up to $\bar{q}q\bar{q}q$ contributions, but fails for higher Fock state components [37]. The reason has to do with an ambiguity on what states should be considered colour irreducible, *i.e.* those in which all constituents are needed to screen the source, without additional constituents forming a colour singlet by themselves. Our analysis faces, once more, the difficulties in making a clear cut definition of a hadronic state out of multiparton states.

The Polyakov loop can be treated in a similar way

$$\begin{aligned}\frac{1}{N_c}\langle \mathrm{Tr}_c \Omega\rangle &= 2N_f \int \frac{d^3x\, d^3p}{(2\pi)^3} e^{-E_p/T} \frac{1}{N_c} \underbrace{\left\langle \mathrm{Tr}_c\Omega(\vec{x}_0)\mathrm{Tr}_c\Omega^\dagger(\vec{x})\right\rangle_G}_{e^{-\sigma|\vec{x}_0-\vec{x}|/T}} + \ldots \\ &= \frac{2N_f}{N_c}\int \frac{d^3x\, d^3p}{(2\pi)^3} e^{-H(\vec{x},\vec{p})/T} \to \frac{2N_f}{N_c}\sum_n e^{-\Delta_n/T}\,,\end{aligned} \tag{102}$$

where we have quantized the heavy–light ground state system as

$$H(p,x)\psi_n = \left(\sqrt{p^2+m_q^2} + \sigma r\right)\psi_n = \Delta_n\psi_n\,. \tag{103}$$

In previous works, the quantization of the quark motion was not considered, and as a consequence, we failed to see the connection to the HRG. In particular, we found that $L_T \sim e^{-M_0/T}$ so we proposed to determine the constituent quark mass from an analysis of the Polyakov loop on the lattice at low temperatures[9]. While fits along these lines turned out to provide too large a constituent mass we preferred to keep the $L_T \sim e^{-M_0/T}$ behaviour with a

[9] As we have noted above, in the heavy-quark limit one has $L_T \sim e^{-m_Q/T}$.

suitable proportionality factor [119]. As we have seen here, the Boltzmann factor contains the gap $\Delta$ (the heavy–light meson mass) which according to our discussion above corresponds to *twice* the constituent quark mass, so that $L_T \sim e^{-2M_0/T}$ and now the value for $M_0$ from the lattice is phenomenologically acceptable.

A similar argument holds for the correlation function between Polyakov loops. This requires an assumption for a four-point correlator in the pure gluonic theory which at low temperature we assume to be

$$\left\langle \mathrm{Tr}_c \Omega(\vec{x})^\dagger \mathrm{Tr}_c \Omega(0) \mathrm{Tr}_c \Omega(\vec{x}_1)^\dagger \mathrm{Tr}_c \Omega(\vec{x}_2) \right\rangle_G = e^{-\sigma r/T} e^{-\sigma r_{12}/T} + e^{-\sigma|\vec{x}-\vec{x}_1|/T} e^{-\sigma r_2/T} + e^{-\sigma|\vec{x}-\vec{x}_2|/T} e^{-\sigma r_1/T} \tag{104}$$

and satisfies cluster decomposition properties. This yields a disconnected piece due to the effect of the quark determinant

$$\begin{aligned} \left\langle \mathrm{Tr}_c \Omega(\vec{x}) \mathrm{Tr}_c \Omega^\dagger(0) \right\rangle &= \frac{e^{-\sigma r/T}\left[1 + Z_{\bar{q}q} + \ldots\right] + |\langle \mathrm{Tr}_c \Omega \rangle|^2}{1 + Z_{\bar{q}q} + \ldots} \\ &= e^{-\sigma r/T} + |\langle \mathrm{Tr}_c \Omega \rangle|^2 . \end{aligned} \tag{105}$$

This reproduces the free energy formula Eq. (55) based on a avoided crossing structure of the $\bar{Q}Q$ energy levels, see Fig. 5, and yields the result for $F_1(r,T)$ sketched in Fig. 6.

### *8.5. Gluon models with Polyakov loop*

We may introduce gluon fields besides those involved by the Polyakov line variable. A particularly interesting case is gluodynamics. At one loop, the effective potential has been computed in [126]. More recently, one loop gluon actions with Polyakov loops in the adjoint representation were suggested in Refs. [127–130], where the background gauge for the classical gluon-field was assumed and a Polyakov gauge for the quantum fluctuations in the field. We consider this form of dynamics but keeping our interpretation of a quantum and local Polyakov loop variable. The partition function is

$$Z = \int D\Omega w[\Omega] Z[\Omega] \equiv \langle Z[\Omega] \rangle , \tag{106}$$

where we assume the two-point correlation function to be

$$\langle \mathrm{Tr}_A \Omega(\vec{x}) \mathrm{Tr}_A \Omega(\vec{y}) \rangle = e^{-\sigma_A |\vec{x}-\vec{y}|/T} . \tag{107}$$

According to our previous discussion and foreseeing the quantization of partonic degrees of freedom, we write in compact form the action as follows (see

also [37])

$$\log Z[\Omega] = -\mathrm{Tr}\log\left(1 - e^{-h/T}\right) , \tag{108}$$

where $\mathrm{Tr} = \int d^3x\, \mathrm{Tr}_A \sum_{\lambda=\pm}$ and the single particle Hamiltonian is given by

$$h = p - igA_0(\vec{x}\,) , \qquad \Omega(\vec{x}\,) = e^{igA_0(\vec{x}\,)/T} . \tag{109}$$

The interpretation of the previous formula is that of a particle in a random purely imaginary gluon field with given correlation functions, and it has been written in a way that preserves large gauge invariance in the Polyakov gauge. In the semiclassical approximation, we can replace the quantum mechanical trace as we already did before[10]

$$\log Z[\Omega] = -2\int \frac{d^3x d^3p}{(2\pi)^3} \mathrm{Tr}_A \log\left(1 - e^{-p/T}\Omega(\vec{x}\,)\right) , \tag{110}$$

where the factor 2 comes from the two spin states. In the limit of a classical and global $\Omega$, we get the action of Refs. [127–130]. The similar criticisms on the ambiguities on the choice of group coordinates at the mean field level apply here. The compact notation in Eq. (108) is extremely useful to carry out the partonic expansion analysis at low temperatures, and pursue the mapping to the glueball gas. Thus, we have to compute

$$Z = \left\langle \exp\left[\mathrm{Tr}\log\left(1 - e^{-h/T}\right)\right]\right\rangle \tag{111}$$

in a power expansion of $e^{-h/T}$. At lowest order, we have $\langle \mathrm{Tr}\, e^{-h/T}\rangle = 0$, and the next order yields

$$\begin{aligned} \frac{1}{2}\left\langle \left(\mathrm{Tr}\, e^{-h/T}\right)^2 \right\rangle &= \frac{g^2}{2}\int \frac{d^3x_1 d^3p_1}{(2\pi)^3}\frac{d^3x_2 d^3p_2}{(2\pi)^3} e^{-H(p_1,x_1;p_2,x_2)/T} \\ &\to \mathrm{Tr}_2\, e^{-H_2/T} , \end{aligned} \tag{112}$$

where $H_2$ is the two-gluon Hamiltonian whose spectrum provides the two-gluon glueballs discussed in the previous section, and $\mathrm{Tr}_2$ is the trace in the corresponding two-gluon Hilbert space. Note that the factor $1/2$ corresponds to the correct Boltzmann counting which originates in the quantum statistical mechanics to avoid the Gibbs paradox in the high-temperature limit [131]. Following similar steps as before, we can obtain the gluelump representation of the Polyakov loop in the adjoint representation. One can

[10] Note that we have scalar gluons with 2 spin states. This is *not* 3 spin-1 states nor 2 helicity states.

analyze what happens for higher Fock states since the glueball gas corresponds to having

$$\log Z = -\sum_n \mathrm{Tr}_n \log\left(1 - e^{-H_n/T}\right) , \tag{113}$$

where here $\mathrm{Tr} = \sum_n \mathrm{Tr}_n$ represents the trace over the whole multigluon Hilbert space. Pursuing the low temperature expansion to higher orders, we have checked that up to three gluons included, the mapping with the glueball mass works but ambiguities arise for 4-gluon states, where the possibility of forming separate and weakly interacting 2-gluon glueballs first arises. We are facing again the concept of colour irreducible clusters inside colour neutral states [37] and the very definition of a hadron.

## 9. Conclusions

Quark–hadron duality at finite temperature is the statement that at low temperatures hadrons can be considered a complete basis of states. The naive hadron resonance gas, while simple minded, works well enough at sufficiently high temperatures as to deserve dedicated attention on *why* becomes this picture invalid. This success remains a mystery over the years since Hagedorn first proposed it.

The listed PDG states incorporate currently just the $q\bar{q}$ or $qqq$ states which fit into the conventional quark model, but what is the nature of states that are needed when approaching the crossover from below? As we have seen, saturating at subcritical temperatures requires many hadronic states, and so the excited spectrum involves relativistic effects even for heavy quarks. This point makes relativistic quark models a potential source for investigation of the hadron spectrum from a global and thermodynamic perspective since the number of needed excited states challenges any lattice QCD calculation. Moreover, the hadronic mapping of Polyakov loops in fundamental and higher SU($N_c$) colour group representations allows to deduce multiquark states, gluelumps and hybrid states, containing one or several heavy quark or gluon sources. This goes beyond the models and opens up the possibility of a Polyakov loop spectroscopy including exotics. While the question on *what* is the complete hadronic particle spectrum remains still open, we envisage the possibility of grasping the yet unknown physics of the phase transition by enquiring this question at the lowest possible temperature where the hadron resonance gas picture fails.

One of us (E.R.A.) warmly thanks Michał Praszałowicz for the invitation and for providing a stimulating atmosphere. We also thank Wojtek Broniowski for many discussions and Marco Panero for clarifications. This work has been supported by Plan Nacional de Altas Energías FPA2011-25948, DGI FIS2011-24149, Junta de Andalucía grant FQM-225, Generalitat de Catalunya grant 2014-SGR-1450, Spanish MINECO's Consolider-Ingenio 2010 Programme CPAN (CSD2007-00042) and Centro de Excelencia Severo Ochoa Programme grant SEV-2012-0234. The research of E.M. has been supported by the Juan de la Cierva Program of the Spanish MINECO, and by the European Union under a Marie Curie Intra-European Fellowship (FP7-PEOPLE-2013-IEF).

## REFERENCES

[1] J.B. Kogut *et al.*, *Phys. Rev. Lett.* **50**, 393 (1983).

[2] J. Polonyi *et al.*, *Phys. Rev. Lett.* **53**, 644 (1984).

[3] R.D. Pisarski, F. Wilczek, *Phys. Rev.* **D29**, 338 (1984).

[4] Y. Aoki *et al.*, *Nature* **443**, 675 (2006) [arXiv:hep-lat/0611014].

[5] O. Philipsen, *Prog. Part. Nucl. Phys.* **70**, 55 (2013) [arXiv:1207.5999 [hep-lat]].

[6] W. Florkowski, *Phenomenology of Ultra-Relativistic Heavy-Ion Collisions*, World Scientific, Singapore 2010.

[7] S. Borsanyi *et al.*, *Phys. Lett.* **B730**, 99 (2014) [arXiv:1309.5258 [hep-lat]].

[8] A. Bazavov *et al.* [HotQCD Collaboration], arXiv:1407.6387 [hep-lat].

[9] W. Melnitchouk, R. Ent, C. Keppel, *Phys. Rep.* **406**, 127 (2005) [arXiv:hep-ph/0501217].

[10] B. Lucini, M. Panero, *Phys. Rep.* **526**, 93 (2013) [arXiv:1210.4997 [hep-th]].

[11] P. Gerber, H. Leutwyler, *Nucl. Phys.* **B321**, 387 (1989).

[12] R. Dashen, S.K. Ma, H.J. Bernstein, *Phys. Rev.* **187**, 345 (1969).

[13] R. Venugopalan, M. Prakash, *Nucl. Phys.* **A546**, 718 (1992).

[14] A. Kostyuk *et al.*, *Phys. Rev.* **C63**, 044901 (2001) [arXiv:hep-ph/0004163].

[15] K. Nakamura *et al.* [Particle Data Group], *J. Phys. G* **37**, 075021 (2010).

[16] S. Godfrey, N. Isgur, *Phys. Rev.* **D32**, 189 (1985).

[17] S. Capstick, N. Isgur, *Phys. Rev.* **D34**, 2809 (1986).

[18] A. Bazavov *et al.*, *Phys. Rev. Lett.* **111**, 082301 (2013) [arXiv:1304.7220 [hep-lat]].

[19] P. Huovinen, P. Petreczky, *Nucl. Phys.* **A837**, 26 (2010) [arXiv:0912.2541 [hep-ph]].

[20] T. Sekihara, T. Hyodo, *Phys. Rev.* **C87**, 045202 (2013) [arXiv:1209.0577 [nucl-th]].

[21] V. Begun, M. Gazdzicki, M. Gorenstein, *Phys. Rev.* **C88**, 024902 (2013) [arXiv:1208.4107 [nucl-th]].

[22] E. Ruiz Arriola, W. Broniowski, P. Masjuan, *Acta Phys. Pol. B Proc. Suppl.* **6**, 95 (2013) [arXiv:1210.7153 [hep-ph]].

[23] T. Suzuki *et al.*, *Phys. Lett.* **B347**, 375 (1995) [arXiv:hep-lat/9408003].

[24] G.V. Dunne, K.M. Lee, Ch. Lu, *Phys. Rev. Lett.* **78**, 3434 (1997) [arXiv:hep-th/9612194].

[25] L. Salcedo, *Nucl. Phys.* **B549**, 98 (1999) [arXiv:hep-th/9802071].

[26] G. Boyd *et al.*, *Nucl. Phys.* **B469**, 419 (1996) [arXiv:hep-lat/9602007].

[27] H. Leutwyler, "Deconfinement and Chiral Symmetry", in: Proc. of Workshop on QCD: 20 Years Later 9–13 Jun 1992, Aachen, Germany, ed. P.M. Zerwas, H.A. Kastrup, World Scientific, 1993, pp. 693–716.

[28] D.E. Miller, *Phys. Rep.* **443**, 55 (2007) [arXiv:hep-ph/0608234].

[29] B. Svetitsky, *Phys. Rep.* **132**, 1 (1986).

[30] O. Kaczmarek *et al.*, *Phys. Lett.* **B543**, 41 (2002) [arXiv:hep-lat/0207002].

[31] E. Megias, E. Ruiz Arriola, L. Salcedo, *J. High Energy Phys.* **0601**, 073 (2006) [arXiv:hep-ph/0505215].

[32] E. Gava, R. Jengo, *Phys. Lett.* **B105**, 285 (1981).

[33] O. Kaczmarek, F. Zantow, *Eur. Phys. J.* **C43**, 63 (2005) [arXiv:hep-lat/0502011].

[34] E. Megias, E. Ruiz Arriola, L. Salcedo, *Phys. Rev. Lett.* **109**, 151601 (2012) [arXiv:1204.2424 [hep-ph]].

[35] S. Gupta, K. Huebner, O. Kaczmarek, *Phys. Rev.* **D77**, 034503 (2008) [arXiv:0711.2251 [hep-lat]].

[36] A. Mykkanen, M. Panero, K. Rummukainen, *J. High Energy Phys.* **1205**, 069 (2012) [arXiv:1202.2762 [hep-lat]].

[37] E. Megias, E. Ruiz Arriola, L. Salcedo, *Phys. Rev.* **D89**, 076006 (2014) [arXiv:1311.2814 [hep-ph]].

[38] E. Megias, E. Ruiz Arriola, L. Salcedo, arXiv:1409.0773 [hep-ph].

[39] J.I. Kapusta, *Nucl. Phys.* **B148**, 461 (1979).

[40] S. Borsanyi *et al.*, *J. High Energy Phys.* **1207**, 056 (2012) [arXiv:1204.6184 [hep-lat]].

[41] J. Greensite, *Prog. Part. Nucl. Phys.* **51**, 1 (2003) [arXiv:hep-lat/0301023].

[42] M. Luscher, P. Weisz, *J. High Energy Phys.* **0207**, 049 (2002) [arXiv:hep-lat/0207003].

[43] G.B. West, *Phys. Rev. Lett.* **77**, 2622 (1996) [arXiv:hep-ph/9603316].

[44] F. Coester, *Helv. Phys. Acta* **38**, 7 (1965).

[45] B. Keister, W. Polyzou, *Adv. Nucl. Phys.* **20**, 225 (1991).

[46] B. Keister, W. Polyzou, *Phys. Rev.* **C86**, 014002 (2012) [arXiv:1109.6575 [nucl-th]].

[47] R. Hakim, *Introduction to Relativistic Statistical Mechanics: Classical and Quantum*, World Scientific, 2011.

[48] C. Anzai, Y. Kiyo, Y. Sumino, *Nucl. Phys.* **B838**, 28 (2010) [arXiv:1004.1562 [hep-ph]].

[49] G.S. Bali, *Phys. Rev.* **D62**, 114503 (2000) [arXiv:hep-lat/0006022].

[50] G.S. Bali *et al.* [SESAM Collaboration], *Phys. Rev.* **D71**, 114513 (2005) [arXiv:hep-lat/0505012].

[51] L.D. Landau, E.M. Lifshits, *Quantum Mechanics Non-relativistic Theory*, transl. from Russian by J.B. Sykes, J.S. Bell, Pergamon Press, 1965.

[52] R.F. Dashen, G.L. Kane, *Phys. Rev.* **D11**, 136 (1975).

[53] O. Kaczmarek, F. Zantow, *Phys. Rev.* **D71**, 114510 (2005) [arXiv:hep-lat/0503017].

[54] E. Ruiz Arriola, L. Salcedo, E. Megias, *Acta Phys. Pol. B Proc. Suppl.* **6**, 953 (2013) [arXiv:1304.2245 [hep-ph]].

[55] A. Bazavov *et al.*, *Phys. Rev.* **D85**, 054503 (2012) [arXiv:1111.1710 [hep-lat]].

[56] S. Borsanyi *et al.* [Wuppertal–Budapest Collaboration], *J. High Energy Phys.* **1009**, 073 (2010) [arXiv:1005.3508 [hep-lat]].

[57] R. Hagedorn, *Nuovo Cim. Suppl.* **3**, 147 (1965).

[58] W. Broniowski, W. Florkowski, *Phys. Lett.* **B490**, 223 (2000) [arXiv:hep-ph/0004104].

[59] W. Broniowski, W. Florkowski, L.Y. Glozman, *Phys. Rev.* **D70**, 117503 (2004) [arXiv:hep-ph/0407290].

[60] T.D. Cohen, V. Krejcirik, *J. Phys. G* **39**, 055001 (2012) [arXiv:1107.2130 [hep-ph]].

[61] K. Johnson, *Acta Phys. Pol. B* **6**, 865 (1975).

[62] J.I. Kapusta, *Phys. Rev.* **D23**, 2444 (1981).

[63] E. Ruiz Arriola, W. Broniowski, arXiv:1110.2863 [hep-ph].

[64] P. Masjuan, E. Ruiz Arriola, W. Broniowski, *Phys. Rev.* **D85**, 094006 (2012) [arXiv:1203.4782 [hep-ph]].

[65] P. Masjuan, E. Ruiz Arriola, W. Broniowski, *Phys. Rev.* **D87**, 118502 (2013) [arXiv:1305.3493 [hep-ph]].

[66] P. Masjuan, E. Ruiz Arriola, W. Broniowski, *Phys. Rev.* **D87**, 014005 (2013) [arXiv:1210.0760 [hep-ph]].

[67] G. Karl, J.E. Paton, *Phys. Rev.* **D60**, 034015 (1999) [arXiv:hep-ph/9904407].

[68] Y. Simonov, *Nucl. Phys.* **B592**, 350 (2001) [arXiv:hep-ph/0003114].

[69] P. Guo *et al.*, *Phys. Rev.* **D77**, 056005 (2008) [arXiv:0707.3156 [hep-ph]].

[70] K. Marsh, R. Lewis, *Phys. Rev.* **D89**, 014502 (2014) [arXiv:1309.1627 [hep-lat]].

[71] H.B. Meyer, arXiv:hep-lat/0508002.

[72] E. Gregory *et al.*, *J. High Energy Phys.* **1210**, 170 (2012) [arXiv:1208.1858 [hep-lat]].

[73] V. Mathieu, N. Kochelev, V. Vento, *Int. J. Mod. Phys.* **E18**, 1 (2009) [arXiv:0810.4453 [hep-ph]].

[74] M. Jacob, G. Wick, *Ann. Phys.* **7**, 404 (1959).

[75] T. Barnes, *Z. Phys.* **C10**, 275 (1981).

[76] V. Mathieu, F. Buisseret, C. Semay, *Phys. Rev.* **D77**, 114022 (2008) [arXiv:0802.0088 [hep-ph]].

[77] F. Buisseret, *Phys. Rev.* **D79**, 037503 (2009) [arXiv:0902.1028 [hep-ph]].

[78] V. Mathieu, *PoS* **QCD-TNT09**, 024 (2009) [arXiv:0910.4855 [hep-ph]].

[79] C.J. Morningstar, M.J. Peardon, *Phys. Rev.* **D60**, 034509 (1999) [arXiv:hep-lat/9901004].

[80] A. Szczepaniak *et al.*, *Phys. Rev. Lett.* **76**, 2011 (1996) [arXiv:hep-ph/9511422].

[81] A.P. Szczepaniak, E.S. Swanson, *Phys. Lett.* **B577**, 61 (2003) [arXiv:hep-ph/0308268].

[82] J. Meyers, E.S. Swanson, *Phys. Rev.* **D87**, 036009 (2013) [arXiv:1211.4648 [hep-ph]].

[83] E. Swanson, *Acta Phys. Pol. B Proc. Suppl.* **6**, 859 (2013).

[84] P. Bicudo, *Phys. Rev.* **D76**, 094005 (2007) [arXiv:hep-ph/0703114].

[85] J. Caro, E. Ruiz Arriola, L. Salcedo, *J. Phys. G* **22**, 981 (1996) [arXiv:nucl-th/9410025].

[86] M. Cardoso, P. Bicudo, *Phys. Rev.* **D78**, 074508 (2008) [arXiv:0807.1621 [hep-lat]].

[87] V. Mathieu, C. Semay, B. Silvestre-Brac, *Phys. Rev.* **D77**, 094009 (2008) [arXiv:0803.0815 [hep-ph]].

[88] E. Megias, E. Ruiz Arriola, L. Salcedo, *Phys. Rev.* **D80**, 056005 (2009) [arXiv:0903.1060 [hep-ph]].

[89] H.B. Meyer, *Phys. Rev.* **D80**, 051502 (2009) [arXiv:0905.4229 [hep-lat]].

[90] F. Buisseret, G. Lacroix, *Phys. Lett.* **B705**, 405 (2011) [arXiv:1105.1092 [hep-ph]].

[91] G. Lacroix *et al.*, *Phys. Rev.* **D87**, 054025 (2013) [arXiv:1210.1716 [hep-ph]].

[92] P.N. Meisinger, T.R. Miller, M.C. Ogilvie, *Phys. Rev.* **D65**, 034009 (2002) [arXiv:hep-ph/0108009].

[93] O. Andreev, *Phys. Rev. Lett.* **102**, 212001 (2009) [arXiv:0903.4375 [hep-ph]].

[94] R.D. Pisarski, *Prog. Theor. Phys. Suppl.* **168**, 276 (2007) [arXiv:hep-ph/0612191].

[95] E. Megias, E. Ruiz Arriola, L. Salcedo, *Indian J. Phys.* **85**, 1191 (2011) [arXiv:0805.4579 [hep-ph]].

[96] E. Megias, E. Ruiz Arriola, L. Salcedo, *Nucl. Phys. Proc. Suppl.* **186**, 256 (2009) [arXiv:0809.2044 [hep-ph]].

[97] E. Megias, E. Ruiz Arriola, L. Salcedo, *Phys. Rev.* **D81**, 096009 (2010) [arXiv:0912.0499 [hep-ph]].

[98] M. Panero, *Phys. Rev. Lett.* **103**, 232001 (2009) [arXiv:0907.3719 [hep-lat]].

[99] S. Datta, S. Gupta, *Phys. Rev.* **D82**, 114505 (2010) [arXiv:1006.0938 [hep-lat]].

[100] J.O. Andersen *et al.*, *Phys. Rev.* **D84**, 087703 (2011) [arXiv:1106.0514 [hep-ph]].

[101] U. Gursoy *et al.*, *Nucl. Phys.* **B820**, 148 (2009) [arXiv:0903.2859 [hep-th]].

[102] E. Megias, H. Pirner, K. Veschgini, *Phys. Rev.* **D83**, 056003 (2011) [arXiv:1009.2953 [hep-ph]].

[103] F. Zuo, *J. High Energy Phys.* **1406**, 143 (2014) [arXiv:1404.4512 [hep-ph]].

[104] C. Christov, E. Ruiz Arriola, K. Goeke, *Acta Phys. Pol. B* **22**, 187 (1991).

[105] E. Megias, E. Ruiz Arriola, L. Salcedo, *Phys. Rev.* **D74**, 065005 (2006) [arXiv:hep-ph/0412308].

[106] P.N. Meisinger, M.C. Ogilvie, *Phys. Lett.* **B379**, 163 (1996) [arXiv:hep-lat/9512011].

[107] K. Fukushima, *Phys. Lett.* **B591**, 277 (2004) [arXiv:hep-ph/0310121].

[108] C. Ratti, M.A. Thaler, W. Weise, *Phys. Rev.* **D73**, 014019 (2006) [arXiv:hep-ph/0506234].

[109] C. Sasaki, B. Friman, K. Redlich, *Phys. Rev.* **D75**, 074013 (2007) [arXiv:hep-ph/0611147].

[110] M. Ciminale *et al.*, *Phys. Rev.* **D77**, 054023 (2008) [arXiv:0711.3397 [hep-ph]].

[111] G.A. Contrera, D. Gomez Dumm, N.N. Scoccola, *Phys. Lett.* **B661**, 113 (2008) [arXiv:0711.0139 [hep-ph]].

[112] B.J. Schaefer, J.M. Pawlowski, J. Wambach, *Phys. Rev.* **D76**, 074023 (2007) [arXiv:0704.3234 [hep-ph]].

[113] P. Costa *et al.*, *Phys. Rev.* **D79**, 116003 (2009) [arXiv:0807.2134 [hep-ph]].

[114] H. Mao, J. Jin, M. Huang, *J. Phys. G* **37**, 035001 (2010) [arXiv:0906.1324 [hep-ph]].

[115] Y. Sakai *et al.*, *Phys. Rev.* **D82**, 076003 (2010) [arXiv:1006.3648 [hep-ph]].

[116] A. Radzhabov *et al.*, *Phys.Rev.* **D83**, 116004 (2011) [arXiv:1012.0664 [hep-ph]].

[117] T. Zhang, T. Brauner, D.H. Rischke, *J. High Energy Phys.* **06**, 064 (2010) [arXiv:1005.2928 [hep-ph]].

[118] E. Megias, E. Ruiz Arriola, L. Salcedo, *Phys. Rev.* **D74**, 114014 (2006) [arXiv:hep-ph/0607338].

[119] E. Megias, E. Ruiz Arriola, L. Salcedo, *PoS* **JHW2005**, 025 (2006) [arXiv:hep-ph/0511353].

[120] E. Megias, E. Ruiz Arriola, L. Salcedo, *AIP Conf. Proc.* **892**, 444 (2007) [arXiv:hep-ph/0610095].

[121] E. Megias, E. Ruiz Arriola, L. Salcedo, *Eur. Phys. J.* **A31**, 553 (2007) [arXiv:hep-ph/0610163].

[122] J. Braun, H. Gies, J.M. Pawlowski, *Phys. Lett.* **B684**, 262 (2010) [arXiv:0708.2413 [hep-th]].

[123] J. Braun *et al.*, *Phys. Rev. Lett.* **106**, 022002 (2011) [arXiv:0908.0008 [hep-ph]].

[124] J. Langelage, O. Philipsen, *J. High Energy Phys.* **1004**, 055 (2010) [arXiv:1002.1507 [hep-lat]].

[125] E. Ruiz Arriola, E. Megias, L. Salcedo, *AIP Conf. Proc.* **1520**, 185 (2013) [arXiv:1207.4875 [hep-ph]].

[126] N. Weiss, *Phys. Rev.* **D24**, 475 (1981).

[127] P.N. Meisinger, M.C. Ogilvie, T.R. Miller, *Phys. Lett.* **B585**, 149 (2004) [arXiv:hep-ph/0312272].

[128] M. Ruggieri *et al.*, *Phys. Rev.* **D86**, 054007 (2012) [arXiv:1204.5995 [hep-ph]].

[129] C. Sasaki, K. Redlich, *Phys. Rev.* **D86**, 014007 (2012) [arXiv:1204.4330 [hep-ph]].

[130] C. Sasaki, *Acta Phys. Pol. B Proc. Suppl.* **7**, 107 (2014) [arXiv:1312.3818 [hep-ph]].

[131] K. Huang, *Statistical Mechanics*, Addison Wesley & Sons, New York 1987.